

# Peer review status:

This is a non-peer-reviewed preprint submitted to EarthArXiv.This manuscript has been submitted to Elementa: Science of the Anthropocene.

Earth ArXiv version 3.0

# A Controlled Release Experiment For Investigating Methane Measurement Performance at Landfills

Rafee Iftakhar Hossain 1\*, Pylyp Buntov 1, Yurii Dudak 1, Rebecca Martino 1, Chelsea Fougere 1, Shadan Naseridoust 2, Evelise Bourlon 1, Martin Lavoie 1, Afshan Khaleghi 2, Chelsie Hall 1, and David Risk 1 Department of Earth and Environmental Sciences, St Francis Xavier University, Antigonish, Nova Scotia, Canada

2 Faculty of Engineering and Applied Sciences, Memorial University of Newfoundland, St. John's, Newfoundland and Labrador, Canada

\*Corresponding author: Rafee Iftakhar Hossain (rhossain@stfx.ca)

# A controlled release experiment for investigating

# methane measurement performance at landfills

- Rafee Iftakhar Hossain<sup>1\*</sup>, Pylyp Buntov<sup>1</sup>, Yurii Dudak<sup>1</sup>, Rebecca Martino<sup>1</sup>, Chelsea
- 4 Fougère<sup>1</sup>, Shadan Naseridoust<sup>2</sup>, Evelise Bourlon<sup>1</sup>, Martin Lavoie<sup>1</sup>, Afshan Khaleghi<sup>2</sup>,
- 5 Chelsie Hall<sup>1</sup>, and David Risk<sup>1</sup>

- <sup>1</sup>Department of Earth and Environmental Sciences, St Francis Xavier University, Antigonish, Nova Scotia, Canada
- 8 2Faculty of Engineering and Applied Sciences, Memorial University of Newfoundland, St. John's, Newfoundland and
- 9 Labrador, Canada
- 10 \*rhossain@stfx.ca

#### **ABSTRACT**

We assessed the performance of various methane measurement solutions in landfill applications. A measurement solution is defined as a system or market offering that quantifies and/or localizes emissions. Our study involved full-scale multipoint- and area-source (dispersed) controlled releases of methane from the ground surface of a closed 25-hectare landfill with collection system and a background emission rate of 24 kg/hr. Most quantification methods performed well, but the truck-based Tracer Correlation method performed the best with an uncertainty of ±20%. Drone flux plane methods also performed well with an uncertainty of ±34% with very few outliers in the best-case scenario. For leak detection, aerial LiDAR demonstrated a 100% detection probability down to the lowest emission rates whereas drone column sensors emulating EPA 21 Surface Emissions Monitoring (SEM) were 100x less sensitive. Continuous sensors, trucks, and other methods were also assessed. Results indicate that many of the current quantification methods are effective, and potentially more accurate than first-order decay models, though they still need to be applied in a replicated fashion for robust site level estimates. Detection outcomes were variable, and questions remain, such as how the evaluated methods would compare the against regulatory SEM method, the impact of spacing and trigger thresholds (which differ regionally in regulation), and what detection level is actually necessary for effective landfill gas management. This site provides a future test bed for answering

these other questions.

#### Introduction

Methane is a potent greenhouse gas, with a global warming potential approximately 81 times greater than CO<sub>2</sub> over 20 years. Major anthropogenic sources of methane include oil and gas production and distribution, agriculture, and waste disposal. Within the waste sector, reducing methane emissions from landfills could reduce anthropogenic emissions up to 500 Mt CO<sub>2</sub>e by 2030 at negative cost (Goldsmith et al., 2011; Nisbet et al., 2020), making the waste sector one of the most economically attractive pathways to reducing methane emissions globally.

To effectively reduce methane emissions from landfills, it is important to accurately measure emission rates. However, reported rates of landfill methane emissions are currently unreliable due to several challenges such as temporal and spatial variability (Mønster et al., 2019), unknown operational details, data scarcity, and prediction model errors exacerbated by the fact that model input parameters such as waste composition can be poorly documented. It is not a surprise that emission estimates might be significantly underestimated in government national inventories (Scarpelli et al., 2024). Directly measuring methane emissions from landfills is an important step in reducing emission estimate uncertainty, helping develop strategies to mitigate emissions, and assessing the effectiveness of landfill gas collection systems (Yang et al., 2023).

The rapid push to reduce methane emissions in the oil and gas sector has led to innovations, some of which have been adopted in the waste sector. However, the average landfill is more than 100 times larger than the typical oil and gas site, emits significantly more, has mounded topography that produces complex wind patterns (Thorpe et al., 2021), and is subject to environmentally-driven variations. To be effective in the waste sector, methane measurement methods used in oil and gas must cope with these different spatial scales and levels of complexity. Modern direct measurement solutions, such as satellites (Mønster et al., 2019), aircraft (Mønster et al., 2019), drones (Daugėla et al. 2020), and mobile sensors (McHale et al. 2019) may detect and consistently quantify methane emissions but many remain untested.

Controlled release experiments can help evaluate and improve measurement solutions but need to be implemented at full scale for realism. Most controlled releases to date (e.g. Chen et al., 2024; Ilonze et al., 2024; Blume et al., 2024; Sherwin et al., 2024) have focused on point sources characteristic of oil and gas, and experiments in landfill settings (Babilotte et al., 2010) predate many newer measurement methods.

In this study, we used controlled releases of methane in a landfill environment to assess the performance of

14 different solutions that can quantify and/or detect landfill methane emissions. We define a solution as a method or system, potentially combined with a specific business model, which quantifies and/or localizes methane emissions at landfills. Our efforts will enhance the overall understanding of methane emissions at landfills and inform the development of more effective monitoring strategies.

#### **Methods**

#### **Site Characteristics**

We conducted our study at the Petrolia landfill in Petrolia, Ontario (42°52'19"N, 82°7'14"W), which has been owned and operated by Waste Management (WM) Canada since 1990. After decades of operation, the operators closed the site to new waste in June 2016. The 26.02 ha (Figure 1) site is capped both with clay and geomembrane providing excellent integrity, is covered in 1 m of topsoil, and seeded. An effective landfill gas collection system draws ~400 kg/hr of gas to an electrical generation facility in the northwest corner of the landfill. Since the site has a high integrity cap (impermeable geotextile, overlain by 1 m clay, overlain by 1-2 m soil), and effective gas collection system, residual ("background") site emissions are low, which is of high benefit to an experiment like this because we can be certain that most of the emissions will originate from purposeful controlled releases on site. The Petrolia landfill's topography is typical, which is also important for study realism. The cells slope away from the center, and the highest point of the landfill is about 35 m above the outer edges and the rural surrounding region. The land surrounding the site is flat and is used as cropland or covered with trees. A public road network provides access around the site, though at some distance depending on direction. A small active oil production tank battery is located about 900 m northeast and was a competing source of methane emissions for any measurement solution in our study that measured emissions downwind.

#### Background emission rates uncertainty estimation

The ideal landfill controlled-release site would mimic real topography and emissions scales without producing its own emissions. The selected closed landfill approximates this: steep relief, realistic scale, and unusually low residual fluxes. Normally landfill covers are either geotextile or clay, but unusually this site is capped using both approaches, and also with >1.5 m soil. The cap is underlain by a vertical well landfill gas collection system operates at negative pressure. A natural landform (e.g., drumlin) could have eliminated residual emissions, but suitable, accessible sites were impractical. Allowing minor background emissions is therefore a small tradeoff for otherwise optimal conditions.

Surface emission mapping from walking surveys confirmed the absence of detectable landfill emissions within the defined search area (Figure S9). However, some smaller background emissions were carefully characterized before and during the experiment. Point sources were identified at several leachate system manhole access points, at the flare associated with the waste generation facility, and from localized soil areas. The general areas of these emission sources is presented in Figure S1. Importantly, all background emission sources were located outside the defined experimental search area, and therefore the issue of background emissions only affected measurement solutions used beyond the search area, for example from roads outside the landfill. While these sources contributed to overall site emissions, they primarily affected measurements from downwind, truck-based solutions operating beyond the controlled test boundary. Background emissions were therefore added to controlled release values only where needed. To quantify background emissions, we applied two independent methods, using different datasets, analytical approach, incorporating different measurement methodologies to build evidence. These methods, including input data, and resultant plots, are described at length in the Supplement, section (Background Emissions – Rates and Locations). Method 1 involved Mobile Tracer Correlation (TruckTC) measurements, between controlled releases when the release system was inactive, which yielded a mean background emission rate of 24.4 kg/hr ( $\sigma$  = 8.8, n = 9). The measurements were conducted over several days, incorporating any natural fluctuations. Method 2 involved an independent regression-based method using datasets submitted by TruckTC and LiDAR (incorporating wind corrections) during the controlled release experiments, where background emissions were not added, and where a yintercept value for each should predict the background emissions. TruckTC and wind-corrected LiDAR were the highest performing solutions in the experiments therefore offered useful estimates. Method 2 v-intercept results from both vendors produced similar estimates: 19.4 kg/hr for TruckTC (R<sup>2</sup> = 0.8, n = 27) and 21.66 kg/hr for AirLiDAR G-2 flux planes (R<sup>2</sup> = 0.77, n = 9). The close agreement across Method 1 and Method 2 approaches indicates that uncertainties in background characterization were low. Comparing background emission rates (including combustion slip from the generation facility) to gas burned for power yields a collection efficient estimate of 98–99% which far exceeds normal performance standards. The high methane collection performance, and low level of background emissions onsite, minimizes the tradeoffs of using a real landfill site for these experiments. As stated earlier, background emission estimates were applied only in the case of evaluating measurement solutions that operated at fence-line or beyond.

113

86

87

88

89

90

91

92

93

94

95

96

97

98

99

100

101

102

103

104

105

106

107

108

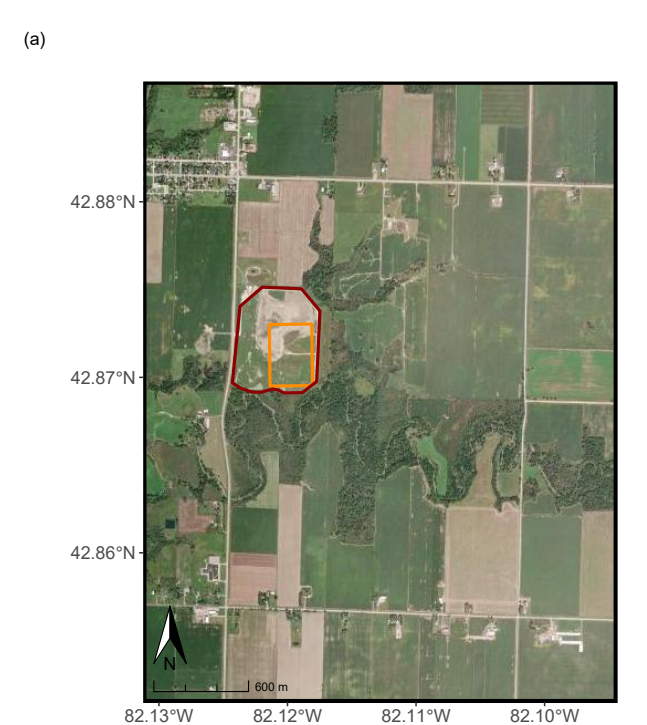
109

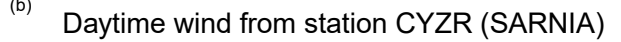
110

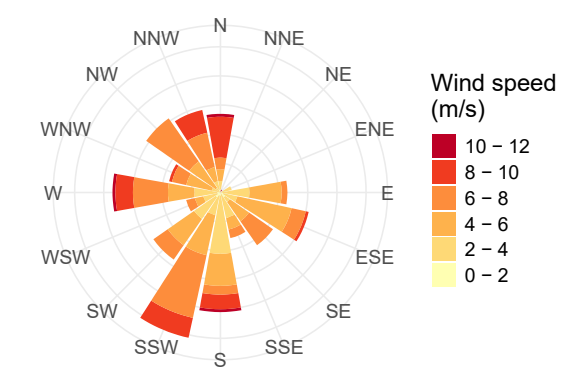
111

112

114







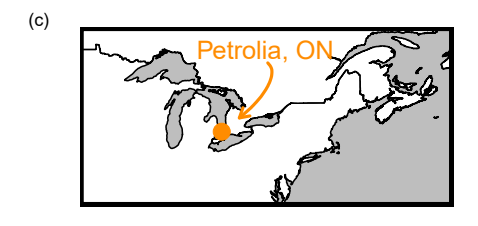


Figure 1. Petrolia location and study area. Panel (a) shows the landfill outlined in red. The experimental study area containing the release points is outlined in orange, and the road network is visible. Panel (b) shows the wind rose for November 2023 from data measured at the nearby Sarnia airport. Panel (c) shows the general location of the Petrolia landfill, near the United States-Canada border and toward the southern end of the Great Lakes area.

#### Multi-Point Controlled Release Pipeline System and Supplementary Measurements

The controlled release system for our study was comprised of a 600 m non-permanent aboveground polyethylene pipeline network inside a 10-ha search area (Figure 1). The pipeline and release system fed a series of 10 surface and shallow subsurface release points at various locations across the search zone. Eight point sources were mounted flush with ground level, and two release points were dispersed gas sources that consisted of perforated tubes sitting just below the surface over 170 m<sup>2</sup>. The point sources could support release rates up to 500 l/min, or 19 kg/hr each, and the perforated tubes area dispersed sources could each emit at 3000 l/min, or 119 kg/hr. The total distance between the extreme ends of the point- and area-release networks was 400 m. All release nodes were controlled with freshly calibrated Alicat MCR ATEX-rated flow controllers (Alicat Scientific, 2025) in black plastic containers, connected to the pipeline network at seven locations. We included several on/off valves to divert flow to

the 10 release points so that each flow controller could monitor and regulate each release source in real-time. Maximum release rates were mainly governed by the number and types of flowmeters available for the study. The total theoretical release capacity for the system was 390 kg/hr but operating permits only allowed up to 300 kg/hr in this set of experiments. With a standard accuracy of ±0.6% of reading or ±0.1% of full scale (500l/min or 3000 l/min), flow rate data were collected every 1 second. We controlled the flow controllers remotely from a laptop with a user interface and that was in a trailer at the end of each downstream branch of the mini-pipeline gas transfer system. For permitting reasons, landfill gas could not be released for this study. A bulk CNG trailer (Hexagon Lincoln Titan 4) supplied natural gas composed of 94.5% methane, 4.5% ethane, 0.09% propane, 0.4% nitrogen, and 0.4% carbon dioxide, and a Certarus Pressure Reduction System (PRS) decompressed the gas on site. Gas composition data was provided by Certarus and a single gas trailer was used for the entire duration of the study. Methane flow rate calculations considered the gas composition. We ensured that the entire landfill surface was mowed before the experiment and that the grass was trimmed near the release elements. Figure S8 shows the map of the search area and release infrastructure.

In addition to the pipeline system, we erected and maintained three meteorological stations for the experiment, two of which were located at the base of the landfill near the northwest and southwest corners and another near the central landfill peak. The meteorological stations consisted of Metsens500 and Metsens200 compact ultrasonic weather sensors that measured wind speed and direction, temperature, relative humidity, and barometric pressure, logging data at 1-minute intervals to a Campbell Scientific CR6 datalogger. The Metsens500 was purchased new for the experiments and used factory calibrations.

#### **Experimental Protocol**

We based our experimental protocol on a previous survey protocol developed by the Methane Emissions

Technology Evaluation Center (METEC) at Colorado State University. METEC's basic protocol validates oil and gas emission measurement solutions using blind controlled releases (Sonderfeld et al. 2017; Bell et al. 2023; Mbua et al. 2023; Day et al. 2024; Ilonze et al. 2024). We modified the METEC protocol to suit landfill methane measurements; instead of just point sources, we defined multiple point sources and source emission areas.

Furthermore, to suit our controlled release study, protocol changes included: separately classifying point and area source releases, differentiating between detection and quantification methods and defining metrics for each, and removing oil and gas terminology.

Participants deployed their measurement solutions to localize or quantify emissions, with certain solutions performing both functions. To evaluate how well the quantification methods estimated emissions, we first defined the geographic boundary of the survey (whole site, or release area only) to determine if background emissions should be added to the metered totals. Participants were provided a release schedule ahead of their participation slots and any changes to the schedule was communicated via email or Telegram and there was approximately a 5-10 minute pause in between experiments. We compared the measured rate estimates (kg/hr) to the sum of the average flowmeter values from our release experiments, plus the background emissions when applicable. To evaluate how well methods detected emissions, we assigned true positives or false positives based on a 20 m x 20 m box surrounding each release point (to account for GPS uncertainty). We considered detected leaks outside the boxes to be false positives, and we classified undetected leaks as false negatives, and so on. Overall, we released 3030 kg of gas over 9 days. We compared the flow rate data from the flow controllers to the end-of-day gas use report from the pressure reduction trailer that the trailer software generated. When we compared the amount of gas released between the flow controllers and the pressure reduction report, the difference was always less than 5% between the two. The difference of up to 5% was calculated between the flow controllers and PRS trailer due to the standard temperature and pressure values for each flow controller. Alicat flow controllers reported standardized volumetric flow rates with the default STP (standard temperature and pressure) of 25°C and 1 atm whereas the flow controller in the PRS reported standardized volumetric flow rates with the default STP of 15.6 ° C and 1 atm. To be consistent with rate comparison (actual vs reported) rates from alicat flow controllers were compared against reported rates from participants. Details on flow rates during each experiment is provided in the Supplement.

183

184

185

186

187

188

189

190

191

192

163

164

165

166

167

168

169

170

171

172

173

174

175

176

177

178

179

180

181

182

Two weeks after making measurements, the participants submitted their measured estimates for evaluation. Participants using a quantification method provided their rate estimates in kg/hr, and those participants using a detection method provided the coordinates of detected leaks. After the first round of submissions, participants resubmitted their data, this time considering the effects of the in situ meteorological data to determine if the experiment would benefit from in situ wind measurements. Participants were free to include/exclude measurements depending on their quality control protocols. We lack an accurate accounting of how many times participants refrained from taking measurements owing to meteorology, but certainly some wind conditions were unsuitable for flying drones, and persistent cloud reduced the upward mixing of plumes for crewed aircraft. Meteorological reports are supplied in the Supplementary Information section.

The entire controlled release study involved 71 experiments during November 6, 2023 and November 14, 2023. We conducted all experiments during daylight hours and under conditions that allowed us to function safely, such as releasing gas when wind speeds were above 2 m/s. Before the experiments, we designed and loaded the release rate configurations into the flow controller software. However, onsite personnel could adjust the configuration to accommodate changes in experiment schedules. For each experiment, a plume setup time from 5 to 10 minutes ensured appropriate downwind dispersion. When possible, we asked participants to replicate measurements within the same experiment, so we could evaluate how consistently each solution performed, and we inserted occasional zero-emission experimental design points. Releases lasted only as long as was needed for participants to complete their survey work.

#### **Participating Solutions**

Table 1 lists the 14 methane measurement solutions used by the participants, including our field team. The umbrella term "solution" incorporates measurement platforms, sensors, detecting solutions, estimating algorithms/methods, and field work practice; that is, the entire system a participant used to detect emissions and/or estimate emission rates. Participants were free to include/exclude measurements depending on their quality control protocols. An accurate accounting of how many times participants refrained from taking measurements was not documented, however conditions where methodologies cannot take measurements will be added to the supplementary information section. We anonymously identified each solution-participant combination as a "Participant" and labeled the Participants from "A" to "N", which included the third-party participants and our field team. This allowed us to test related solutions or more broadly methodologies, without targeting individual participants. We asked all participants to submit information on their respective solutions using a standard questionnaire. Table 1 shows that most measurement solutions in this study quantified emissions, two solutions simply detected emissions, and three solutions quantified estimates and detected emissions. We also allowed participants to join a research and development stream ("R&D" in Table 1) that allowed more flexibility in reporting timelines if their solution was not market-ready at the time of our evaluations. Additional information on each solution is provided in the Supplementary Information.

| Identifier | Outcome | Platform   | Sensor                     | Flux Model         | Name     | R&D? |
|------------|---------|------------|----------------------------|--------------------|----------|------|
| Α          | Q       | Truck      | LGR                        | Gaussian           | TruckGP  | No   |
| В          | Q       | Truck      | LICOR                      | Gaussian           | TruckGP  | No   |
| С          | Q       | Drone      | TDLAS Point Sensor         | Flux Plane         | DroneFP  | No   |
| D          | Q       | Drone      | TDLAS Point Sensor         | Flux Plane         | DroneFP  | No   |
| E          | Q       | Truck      | Picarro                    | Tracer Correlation | TruckTC  | No   |
| F          | Q       | Aircraft   | Picarro                    | Flux Plane         | AirFP    | No   |
| G          | Q/D     | Helicopter | AirLiDAR                   | Proprietary        | AirLiDAR | No   |
| Н          | Q/D     | Satellite  | Spectrometer               | Mass Enhancement   | SatME    | No   |
| I          | Q       | Fixed      | EM27                       | Flux Plane         | FixedFP  | Yes  |
| J          | Q       | Fixed      | Metal Oxide Point Sensor   | Gauss/Proprietary  | FixedPS  | Yes  |
| K          | Q       | Fixed      | Metal Oxide Point Sensor   | Gauss/Proprietary  | FixedPS  | Yes  |
| L          | D       | Drone      | Pergam TDLAS Column Sensor | -                  | DroneCS  | No   |
| M          | D       | Drone      | Pergam TDLAS Column Sensor | -                  | DroneCS  | No   |
| N          | Q/D     | Truck      | LGR                        | Lagrangian         | TruckLG  | Yes  |

**Table 1.** Summary of solutions represented in the study. Solutions represented by Q are quantification technologies and solutions represented by D are detection technologies.

Results

#### **Comparing Solutions**

#### Mobile and Drone-Based Solutions: TruckGP, TruckTC, and DroneFP

Figure 2 shows how well the TruckGP, TruckTC, and DroneFP solutions performed. Regression lines for the parity charts were forced through the origin since a regular fit (i.e. with a non-zero y intercept) may represent an inaccurate interpretation. Participants A and B used the same TruckGP method, and both participants underestimated the release rates and generally returned about 60% of the known release rate (Table 2). The author team was solution provider A and N in this category. To maintain a "blind" level of participation we set up internal firewalls between those who collected and processed these measurements, and those who organized and conducted the controlled release study. To offset this lack of independence, we opted to mechanistically disclose all outcomes for all model output (even if we felt they could be outliers), and we also published all raw mobile survey datasets in the archive (see data availability statement). Our results agree with a previous study in which TruckGP measured about 70% of known rates (Fredenslund et al., 2018), indicating potential for systematic bias. TruckTC (Participant E) measurements were comparable to known release rates, with almost no bias. Participant C used the DroneFP method, and the measurements were closer to the parity line than the three truck-based solutions' results. However, Participant D had more spread in their measurements, the mobile truck-based offsite solutions,

TruckTC and TruckGP, offered flexibility and extended duty cycle across weather conditions, and TruckTC and TruckGP could report measurements every day, including on inclement days when drone, aerial, and satellite systems were grounded.

Release rates during this study changed every 50 minutes in most cases, resulting in one or two transects for most experiments using the TruckGP solution. A study by Caulton et al. (2018) showed that increasing the number of transects results in a mean emission rate of higher accuracy, it was recommended that sites should be measured with at least ten transects to reliably constrain atmospheric variability. Reported uncertainties (variances or errors) differed among the solutions. Variance estimates provided by Participants A and B (TruckGP) seemed low, and few overlapped the line of best fit. Uncertainty estimates from Participant E (TruckTC) were realistic and almost all estimates overlapped the line of best fit. Participant C (DroneFP) also reported reasonable variances. Participants B and E (TruckGP and TruckTC, respectively) had similar quantification error levels. However, we note that the largest variations occurred in the afternoon measurements for Participant B, but the largest variations occurred in the morning for Participant E.

Ars et al. (2020) found that the stability class contributes most to uncertainty in TruckGP quantification estimates. Pasquill Stability classification describes dispersion conditions using available meteorological conditions from weather stations (Kahl & Chapman, 2018). After stability class, the greatest contributors of uncertainty to the method are wind direction, wind speed, and source location, with the overall uncertainty reported to be around 75%. With better constraints on atmospheric conditions, the uncertainty decreased to 55% (Ars et al., 2020). In another landfill study using TruckGP, Ravikumar et al. (2019) reported an uncertainty of approximately 30% on emission estimates obtained from distant road measurements. O'Connell et al. (2019) determined the truck-based emission rate uncertainty to be 63% in their controlled release study. The bias of 1.58 and 1.76 in Participant A and B results, respectively, fit into the uncertainty range found by Ars et al. (2020). Using Participant A's data, we averaged successive groups of six measurements from low emission rates to high emission rates, to simulate the effect of including 12 transects (6 measurements x 2 transects) into a single measurement estimate. As expected, these groupings halved the average residuals (departures from the line of best fit) to 13 kg/hr across a range of 25 kg/hr to 200 kg/hr. For TruckGP, we found that better replication would decrease the variance from this solution, and a bias correction or system change would improve accuracy and decrease the bias. Once the improvements were made, the solution would be sufficiently accurate for screening purposes to determine approximate emission levels or to repeat measurements for determining temporal variation at a low cost.

241

242

243

244

245

246

247

248

249

250

251

252

253

254

255

256

257

258

259

260

261

262

263

264

265

266

267

268

269

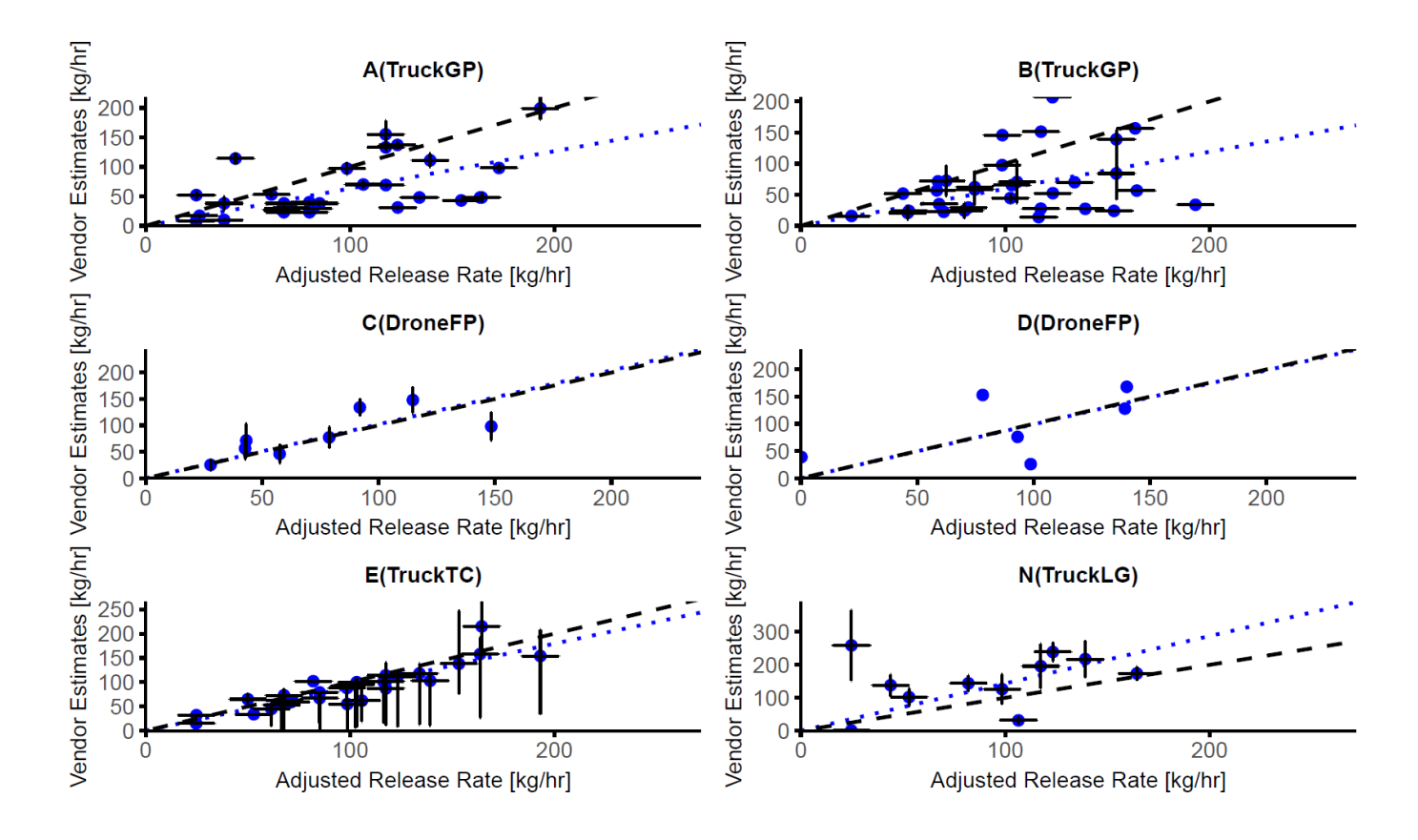


Figure 2. Parity plots of controlled release tests for truck- and drone-based measurements. The dashed lines represent the 1:1 parity relationship. Vertical error bars are based on the upper and lower limits of the measurements provided by the participants. Horizontal error bars were calculated from the uncertainty of the Tracer Correlation method. Blue dotted lines are ordinary least square fits forced through the origin. Bias towards over/underestimating emissions can be observed through the trendline.

In contrast to the other mobile vehicle-based solutions, we found TruckTC to accurately provide rate estimates, and the measurements were close to the parity line with low residuals (Table 2). We could not detect any dependence on the departure of individual measurements and environmental conditions. Previous studies, such as Foster-Witting et al. (2014), noted that TruckTC is relatively insensitive to atmospheric changes.

TruckLG (Participant N) participated as an R&D method, but its performance was promising despite our study being the solution's first trial and the trial being much shorter than the participants would have preferred; that is, on the order of tens of minutes to collect data rather than hours. More work is warranted on this approach under better

conditions and to continue improving it and exploring associated costs and practicality.

Figure 2 shows performance for the two DroneFP solutions. Participant C's estimates were excellent as shown by the parity plot where the data points are in close proximity to the parity line and the trendline shows low bias, but estimates from Participant D were much less predictable. Although the regression line of best fit was statistically significant (p<0.05), there was a substantial departure from the parity line in the Participant D results. Participant D developed the levels of uncertainty for their solution with data from our study; however, the participant expected an uncertainty of 5%, which did not agree with the observed uncertainty in the field. The DroneFP estimates from both participants were less biased for our study than in a previous controlled release study that reported a 37% overestimate bias (Ravikumar et al., 2019). We note, however, that Ravikumar et al., (2019) tested an earlier version of DroneFP. Measurement estimates have improved in recent years, or else landfill controlled-release measurements are better suited to this solution than smaller oil and gas point source releases. Wind speed and error were inversely correlated for Participant C's estimates using the DroneFP method, and the percent error decreased as the wind speed approached 4 m/s to 6 m/s.

Consistent with a review of advanced drone leak detection and quantification methods by Hollenbeck et al. (2021), we found that DroneFP offered accurate emission rate estimates but was sensitive to atmospheric stability. In controlled release testing of flux screens derived from miniature Mid-Wave Infrared TDLAS data collected aboard a quadcopter (Corbett and Smith, 2022), the linear fit between the metered and calculated rates had R<sup>2</sup>=0.8236, which was comparable to the R<sup>2</sup> from Participants C's and D's data: R<sup>2</sup>=0.9201 and R<sup>2</sup>=0.8211, respectively).

# Aerial and Satellite Solutions

The participant using the satellite-based method detected no emissions. Three satellite observations were attempted during the experimental period. All three attempts resulted in a successful acquisition without a detection. Contributing factors for their null detections included release rates not meeting the minimum detection threshold, greater cloud coverage in November, and lower elevation of the sun which resulted in reduced signals for northern sites. Discussions with the participant confirmed that the emissions distribution would have been challenging for their SISEA method to detect. The emission rates were nearly 300 kg/hr, distributed over 10 ha from 10 release points that included two area-based release points. For our release configuration, the minimum detection threshold could not be predicted from the participant's results, but the threshold seemed to exceed 300 kg/hr. Other satellite-based sensors might face similar issues when measuring with the limitations mentioned.

Measurements completed by the Global Airborne Observatory (GAO) also mentions that emissions may not be detected or quantified if rates are below the detection limit which can vary depending on environmental conditions. Furthermore, diffused methane sources can be difficult for satellite sensors to detect (Scarpelli et al., 2024).

Participant F (AirFP method), generally underestimated emission rates compared to the actual release rates. The participant did not classify the measurements as high quality because the meteorological conditions for making accurate measurements had not been met. For the Participant F solution, meteorological conditions must allow for an emission plume to rise and disperse. The preferred conditions under Pasquill stability Class B are wind speed ranging from 2 m/s to 6 m/s, good solar insolation, and limited cloud cover. During Participant F's scheduled measurement times, wind speeds were 7 m/s to 11 m/s, and the sky was nearly overcast. Therefore, the plume flowed beneath the minimum flying altitude and did not rise quickly enough to be measured. Despite the poor conditions, Participant F's measurements related linearly to the actual release rates with an R<sup>2</sup>=0.89. The slope of the line of best fit was 0.67 (Table 2), meaning that Participant F was reporting only 67% of the actual emission rate.

The underestimating bias in Participant F's results compared favorably to Abbadi et al.'s (2024) recent estimates for point source releases. In their study, their measurements strongly correlated to actual rates with an R<sup>2</sup>=0.92 (see Table 2), but they only reported 52% of the actual emission rate. Like MGPEA, AirFP tended to underestimate results, and the estimates would need to be corrected for bias.

The variance estimates that Participant F provided moderately overlapped the line of best fit. A few historic studies measured methane emission fluxes from landfills using the AirFP mass balance approach (e.g., Cambaliza et al. 2017; Allen et al. 2019; Gasbarra et al. 2019; Yong et al. 2024), but to our knowledge, the approach was never validated with a blind controlled methane release test conducted in a landfill. Nonetheless, one controlled release test over a managed agricultural field showed that, under favorable conditions, emissions from the point release source could be quantified by an aerial mass balance approach (using a drone) with an uncertainty of 30% (Morales et al., 2022). Morales et al. (2022) stated that emission rate estimates were on average slightly overestimated under optimal conditions, but they observed a lower average accuracy when they measured emissions under less favorable wind conditions. In another controlled release study, also with a methane point source, Abbadi et al. (2024) showed, that despite a small number of measurements, the aerial mass balance approach could quantify releases above 10 kg/hr.

Figure 3. Parity plots of controlled release tests for aerial measurements and continuous sensor systems. Plots G-1 (AirLiDAR) and G-2 (aerial mass balance) show two separate measurements conducted by the associated participants. Blue data points represent the initial submissions, and the orange data pointsrepresent the revised submissions that considered local meteorological conditions. The bottom three panels show parity plots for the continuous sensor systems Blue hollow points are initial estimates from participants G-1 and G-2, filled orange points are resubmitted estimates.

Participant G used two forms of AirLiDAR quantification that included aggregate emissions during their detection scans (G-1 LIDAR in Figure 3), and they used aerial mass balance screens (G-2 Mass Balance in Figure 3) to quantify methane releases. Both techniques were successful, but the techniques overestimated results. The mass balance estimates overestimated rates more than the AirLiDAR estimates (Table 2). After considering onsite meteorological data, the estimates improved and were closer to actual emissions values in both cases, with the

detection scans and screens overestimating by 43% and 17%, respectively. AirLiDAR quantification for the landfill setting did not achieve the accuracy found in oil and gas settings (Conrad et al., 2023). However, Conrad et al. (2023) reported that the AirLiDAR method performed differently under dark skies and shadows, which produced biases. During the majority of our nine test days, there was cloud cover, so these meteorological biases could have influenced AirLiDAR results.

#### **Continuous Sensor Solutions**

The bottom three panels of Figure 3 show parity plots for continuous emission measurement systems (CEM), all of which were part of the R&D stream. Our study aims to specifically develop CEM sensors and algorithms for landfill emission measurements because continuous sensors are a low-effort way to measure emissions compared to other solutions. In our study, estimates from Participant J were the closest to actual emission values compared to the estimates from other continuous sensor solutions, although uncertainties in Participant J's results were unrealistically large where the upper and lower limit of estimate rates are greater than 300 kg/hr. Due to the small number of sensors available for our study, only a limited set of wind conditions was covered, which might have contributed to the large uncertainty.

The continuous sensors are promising solutions from a cost and variability standpoint, but the sensor total solutions are in the early stages of development for waste sector applications. One of the key strengths of CEM sensors is the ability capture temporal variability of emissions. Emission concentrations are captured by most CEM sensors however more research is required to develop models to calculate flux and site specific device coverage. A controlled release study for oil and gas detection by Chen et al. (2024) focused on detecting and quantifying methane emissions using Continuous Methane Monitoring Technologies, and while some of the solutions implemented in their study were accurate, others produced large numbers of false positives (Chen et al., 2024). However, landfills are very different from oil and gas sites, and landfills challenge these solutions because landfills have complex topographies, multiple source locations, and geographic scales of 80 to 100 times those of oil and gas sites. Landfill-specific controlled release testing and development must be conducted to bring these new continuous systems towards maturity for the waste sector; however, the initial results are promising.

| ID | Name     | Slope(1st) | R <sup>2</sup> (1st) | Slope(2nd) | R <sup>2</sup> (2nd) | Bias  | Residuals<br>StDev as<br>% kg/hr | Dev. from true value % | Reps(n) |
|----|----------|------------|----------------------|------------|----------------------|-------|----------------------------------|------------------------|---------|
| Α  | TruckGP  | 0.66       | 0.77                 | -          | -                    | 1.51  | 47.61                            | 1-160                  | 30      |
| В  | TruckGP  | 0.57       | 0.67                 | -          | -                    | 1.76  | 39.63                            | 1-88                   | 31      |
| С  | DroneFP  | 1.02       | 0.90                 | -          | -                    | 0.98  | 34.71                            | 2-66                   | 8       |
| D  | DroneFP  | 0.99       | 0.82                 | -          | -                    | 1.01  | 61.98                            | 8-96                   | 6       |
| E  | TruckTC  | 0.90       | 0.96                 | -          | -                    | 1.12  | 20.49                            | 3-44                   | 28      |
| F  | AirFP    | 0.68       | 0.89                 | -          | -                    | 1.48  | 23.89                            | 1-77                   | 10      |
| G1 | AirLiDAR | 1.47       | 0.96                 | 1.24       | 0.97                 | 0.81* | 44.64*                           | 6-128*                 | 12      |
| G2 | AirLiDAR | 1.49       | 0.90                 | 1.23       | 0.96                 | 0.82* | 40.67*                           | 7-130*                 | 9       |
| Н  | SatME    | -          | -                    | -          | -                    | -     | -                                | _                      | 0       |
| I  | FixedFP  | 2.43       | 0.64                 | -          | -                    | 0.41  | 975.2                            | 1-3597                 | 14      |
| J  | FixedPS  | 1.40       | 0.79                 | _          | -                    | 0.72  | 96.36                            | 2-306                  | 25      |
| K  | FixedPS  | 0.46       | 0.60                 | _          | -                    | 2.17  | 39.10                            | 5-96                   | 30      |
| N  | TruckLG  | 1.44       | 0.73                 | -          | -                    | 0.70  | 88.34                            | 6-215                  | 11      |

**Table 2.** Methane measurement solution performance metrics during quantification tests. Columns indicating "1st or 2nd sub" refer to data submissions, where the second submission considered ground-based wind data from the onsite meteorological tripods. Bias correction factor is defined as 1/slope, where the factor > 1 shows negative bias and factor < 1 shows positive bias. Background emission rate was added to the flow controller rate for participants taking offsite measurements (A,B,E,F,G2 & N)

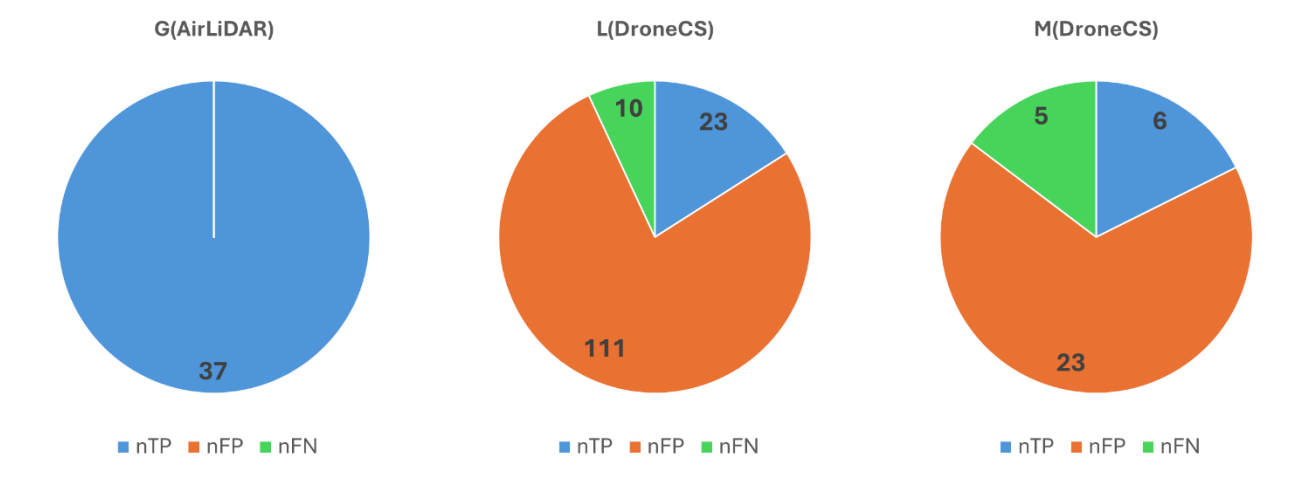
#### **Detection Performance Assessments**

Figure 4 illustrates the total number of true positives, false positives, and false negatives for Participants G, L, and M. True positives are defined as emission point estimates that can be attributed to an emitting source, false positives are emission point estimates that cannot be attributed to an emitting source and false negatives are active sources that were not detected. False positive and negative fractions closer to zero were desirable because they indicate that the solution correctly detected emissions. Participant G (AirLiDAR) detected active emissions 100% of the time with no false positive and false negative readings. Participants L and M used the same drone-mounted TDLAS column sensors in their solutions, and both their results reported a high fraction of false positives. The false positive fraction for participant L was 0.83 and 0.79 for participant M. The false negative fraction for participant L was 0.63 and 0.50 for participant M. False positive emission points are classified as leak estimates outside of the 20 m x 20 m box. Controlled emissions were present in all experiments where drone column sensors participated therefore all false positives can be assumed as localization errors. Although Participants L and M used identical sensors, Participant M was slightly more sensitive to leaks, and we suspect that the difference was due to subtle differences in their work practice. Both participants could not fully deploy their solutions, because a manual ground visit could not be performed to validate potential leak sources identified by the drone-mounted sensor. The study area could only be accessed when gas was not being released. Not being able to validate results likely contributed to the

higher percentage of reported false positives for Participants L and M. Participant N (TruckLG) deployed 1 km to 1.9 km from the landfill's center and could discern leak sources within 100 m, indicating an uncertainty rate of about 15%. Participant N was in the R&D category and future participation may entail being more selective when reporting under non ideal conditions.

For each detection solution that registered readings, we created a statistical curve depicting the probability of detection. We plotted detection results against release rates and wind speed. We found AirLiDAR to be very sensitive to emissions as low as 1 kg/hr with a 100% probability of detection which is consistent with Bell et al. (2022) who found a minimum detection limit of 0.25 (kg/hr)/(m/s) at an altitude of 500 ft AGL.

For DroneCS, the 90% probability of detection was 95.34 kg/hr (Participant L) and 101.88 (Participant M). It is not known how these rates would compare to a traditional walking survey with the same spacing, because, to our knowledge, walking survey measurements have never been validated with controlled release experiments. For walking surveys and DroneCS, survey spacing is likely to affect detection probability at different rates of release. In our study, virtually all true positive DroneCS detections occurred with moderate wind speeds, between 2 m/s and 4 m/s. At 30 m spacing the solution would depend on the flux of emitted gases from the points of release to the transected locations. However, too much wind would dilute the gas plumes below the characteristic EPA21 threshold of 500 ppm that Participants L and M used. With some alterations to their practice (e.g., altering spacing or wind-dependent thresholds) the Participant L and M solutions would likely perform better because their sensor has the potential to detect as little as 0.1 kg/hr with 30 cm spacing from 20 m above ground level. A similar study used DroneCS to detect a release of 4 kg/hr in pipeline surveys (Li et al., 2020), suggesting that the method can perform better. Many landfills are steeply sloped, and these topographical slope changes seemed to affect how DroneCS performed in our study. On the slopes, oblique angles of incidence might have reduced laser returns if no gimbal had been used to maintain a laser path perpendicular to the ground. Compared to slope measurements, true positive measurements were more frequent on flat surfaces.



**Figure 4.** Total number of true positives( nTP), false positives (nFP), and false negatives (nFN) for Participants G, L, and M

#### Discussion

Overall, the quantification results from most of our tested solutions were promising, as shown in Figure 5. Measurement uncertainties for quantifying emissions were lower in this study than have been documented in numerous controlled release studies at oil and gas sites. Presumably the larger size and emission profile of a landfill is a driving factor, since measurement solutions can operate comfortably above minimum detection thresholds. We observed high variability among some participants using FixedPS and DroneFP, which indicated that standardized operating procedures are needed for these methods. We observed very similar results from solutions using TruckGP TruckGP is normally used to measure a landfill site over hours (Kumar et al., 2024), often with replicates over several days (Risk et al., 2025) where the averaging of multiple transects increases the certainty of the emission estimate, which is unlike the situation these solution providers faced in the study where release rates and locations were changing approximately every hour. Ultimately we cannot identify a "best solution" for quantification. For applications like annual inventories, issues like sample size co-determine the outcome. Solutions suited for repetitive use by virtue of low cost, lack of setup time, or lack of environmental limiters, could in theory deliver more accurate annual inventories than highly accurate but infrequently used solutions. For landfills, the issue of sample size is more important than in oil and gas where sites are numerous and measurement variability is naturally averaged out in large survey campaigns. Landfill site-level inventories would perhaps sit as the most challenging

implementation of quantification solutions, as many replicates across seasons would likely be required to average out temporal and measurement variability. Our point here is that even top-performing quantification solutions will not automatically deliver robust inventories. Experimental design of inventory sampling programs is as important as the choice of measurement solution.

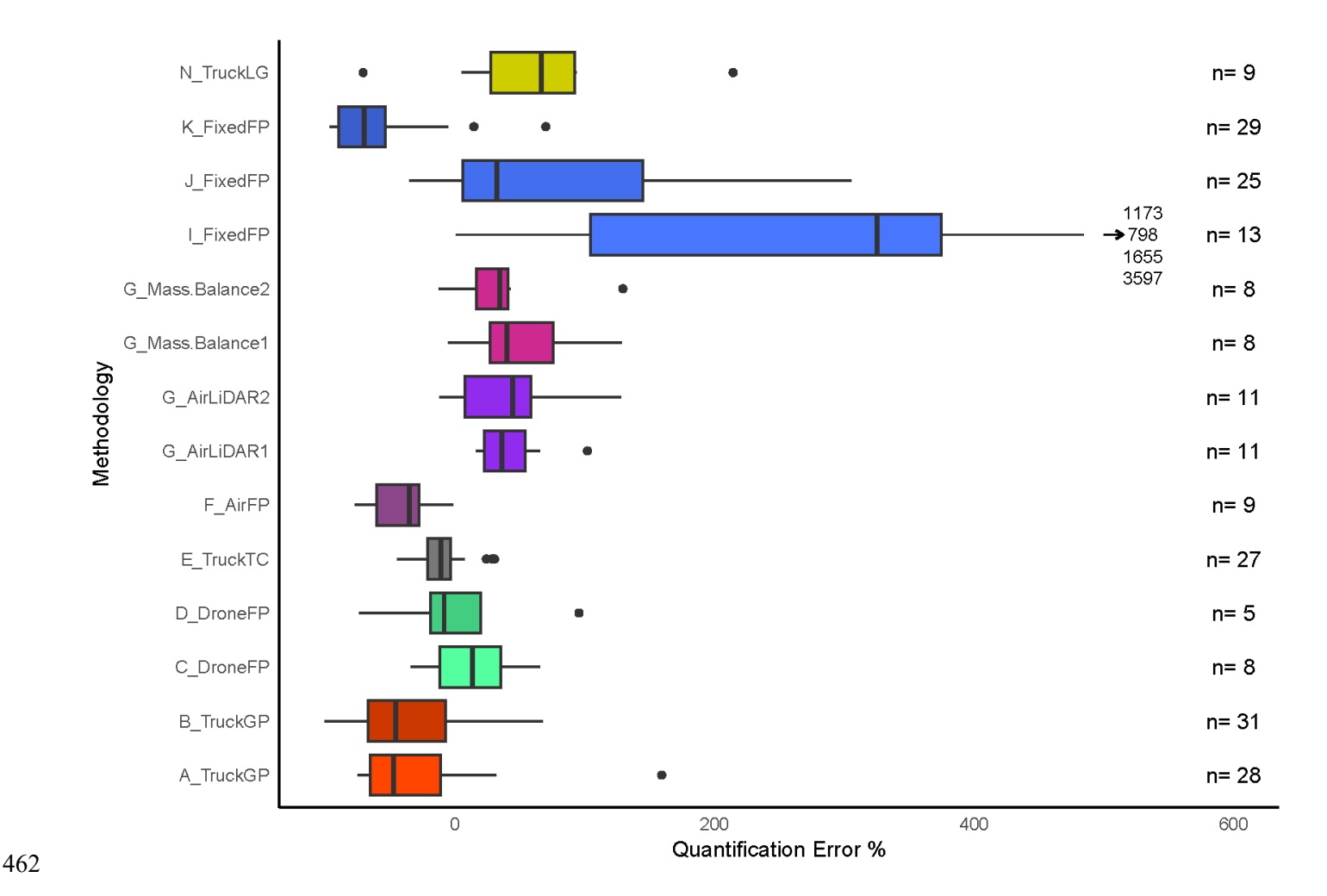


**Figure 5.** Box plot of relative quantification error percentage. In this plot, the x-axis is limited from -100 to 600 to view the most observations, and it should be noted that we received a few submissions with larger errors that are not shown here.

There is pressure to replace walking surveys with repeatable remote methods to reduce injuries on rough terrain (Wu et al., 2023). AirLiDAR performed very well and seems a clear immediate alternative. Drone-based DroneCS solutions did not show high sensitivity towards active emissions points, but future work in controlled release environments may aid in their development. The high percentage of false positives in drone column sensors are due to localization errors where emission points where reported within the search area where there were no presence of active or confounding sources of emissions. Unfortunately, the performance criteria for adoption of any new solutions is uncertain. It is currently impossible to compare them against the incumbent walking EPA21

Surface Emission Monitoring (SEM) solution since its emission rate sensitivity is not known. EPA21 testing is possible in controlled release scenarios and is an important topic for future study since it too may perform differently than expected.

While background emissions at the controlled release site introduced some uncertainty, their effect was minor compared with the much larger reported uncertainties of most measurement teams. Variability in background flux was normally distributed and therefore unlikely to bias team estimates, serving mainly to increase data scatter. A formal propagated uncertainty analysis would be difficult given the inconsistent ways teams reported uncertainty – if they reported uncertainty at all. More informative would be future tests of claimed uncertainties through repeated blind emissions. Ultimately, background emission uncertainties were a reasonable tradeoff given the site's otherwise ideal attributes; other factors, such as wind-field adjustments (e.g., LiDAR offsets), the poor performance of continuous emission systems under complex terrain and multiple sources, or truck underestimates caused by forest flow blocking, played a much larger role in shaping team outcomes. Only the very best-performing systems could plausibly have been affected by the modest background uncertainty; for the rest, larger methodological challenges and uncertainty drivers dominate the outcomes of this experiment.

Our study contributes to the understanding of how different solutions operate and perform in a landfill and dispersed release setting, yet several aspects of our study warrant further exploration. One such topic is the validation of aircraft flux mapper data (Scarpelli et al., 2024) and satellite-based methane measurements (GHGSat, 2024; Carbon Mapper, 2024). These specific solutions report landfill emissions worldwide but have not been fully validated for dispersed source landfill emissions measurement. This study will help operators, regulators, industry and government stakeholders make better-informed decisions regarding landfill emission measurement methods. Additionally, vendors can use the data generated from this research to refine their technologies and enhance their measurement approach for the waste management sector, ultimately contributing to methane reduction.

#### References

Abbadi SHE, Chen Z, Burdeau PM, Rutherford JS, Chen Y, Zhang Z, Sherwin ED, Brandt AR. 2024. Technological maturity of Aircraft-Based methane sensing for greenhouse gas mitigation. Environmental Science & Technology 58:9591–9600. doi:10.1021/acs.est.4c02439

| 502 |   |
|-----|---|
| 503 | Alicat Scientific. (2025, July 15). Laminar DP Mass Flow Controller for Gas - Alicat Scientific.                          |
| 504 | https://www.alicat.com/products/gas-flow/mass-flow-controller/laminar-dp-mass-flow-controllers/                           |
| 505 |   |
| 506 | Allen, G., Hollingsworth, P., Kabbabe, K., Pitt, J. R., Mead, M. I., Illingworth, S., Roberts, G., Bourn, M., Shallcross, |
| 507 | D. E., Percival, C. J. 2019. The development and trial of an unmanned aerial system for the measurement of                |
| 508 | methane flux from landfill and greenhouse gas emission hotspots. Waste Management, 87, 883-892.                           |
| 509 | https://doi.org/10.1016/j.wasman.2017.12.024  |
| 510 |   |
| 511 | Ars S, Vogel F, Arrowsmith C, Heerah S, Knuckey E, Lavoie J, Lee C, Pak NM, Phillips JL, Wunch D. 2020.                   |
| 512 | Investigation of the spatial distribution of methane sources in the Greater Toronto area using mobile gas                 |
| 513 | monitoring systems. Environmental Science & Technology 54:15671–15679. doi:10.1021/acs.est.0c05386                        |
| 514 |   |
| 515 | Babilotte A, Lagier T, Fiani E, Taramini V. 2010. Fugitive Methane Emissions from Landfills: Field Comparison of          |
| 516 | Five Methods on a French Landfill. Journal of Environmental Engineering 136:777–784. doi:10.1061/(asce)ee.1943-           |
| 517 | 7870.0000260  |
| 518 |   |
| 519 | Bell C, Ilonze C, Duggan A, Zimmerle D. 2023. Performance of Continuous Emission Monitoring Solutions under a             |
| 520 | Single-Blind Controlled Testing Protocol. Environmental Science & Technology 57:5794–5805.                                |
| 521 | doi:10.1021/acs.est.2c09235   |
| 522 |   |
| 523 | Bell C, Rutherford J, Brandt A, Sherwin E, Vaughn T, Zimmerle D. 2022. Single-blind determination of methane              |
| 524 | detection limits and quantification accuracy using aircraft-based LiDAR. Elementa Science of the Anthropocene 10.         |
| 525 | doi:10.1525/elementa.2022.00080   |
| 526 |   |
| 527 | Bell CS, Vaughn T, Zimmerle D. 2020. Evaluation of next generation emission measurement technologies under                |
| 528 | repeatable test protocols. Elementa Science of the Anthropocene 8. doi:10.1525/elementa.426                               |
| 529 |   |
| 530 | Blume N, Pernini TG, Dobler JT, Zaccheo TS, McGregor D, Bell C. 2024. Single-blind detection, localization, and           |
| 531 | quantification of methane emissions using continuous path-integrated column measurements. Elementa Science of             |

21/50

| 532 | the Anthropocene 12. doi:10.1525/elementa.2024.00022   |
|-----|--|
| 533 |  |
| 534 | Cambaliza MOL, Bogner JE, Green RB, Shepson PB, Harvey TA, Spokas KA, Stirm BH, Corcoran M. 2017. Field                  |
| 535 | measurements and modeling to resolve m2 to km2 CH4 emissions for a complex urban source: An Indiana landfill             |
| 536 | study. Elementa Science of the Anthropocene 5. doi:10.1525/elementa.145  |
| 537 |  |
| 538 | Caulton, D. R., Li, Q., Bou-Zeid, E., Fitts, J. P., Golston, L. M., Pan, D., Lu, J., Lane, H. M., Buchholz, B., Guo, X., |
| 539 | McSpiritt, J., Wendt, L., & Zondlo, M. A. (2018). Quantifying uncertainties from mobile-laboratory-derived emissions     |
| 540 | of well pads using inverse Gaussian methods. Atmospheric Chemistry and Physics, 18(20), 15145–15168.                     |
| 541 | https://doi.org/10.5194/acp-18-15145-2018  |
| 542 |  |
| 543 | Chen Z, Abbadi SHE, Sherwin ED, Burdeau PM, Rutherford JS, Chen Y, Zhang Z, Brandt AR. 2024. Comparing                   |
| 544 | Continuous Methane Monitoring Technologies for High-Volume Emissions: A Single-Blind Controlled Release Study            |
| 545 | ACS ES&T Air 1:871–884. doi:10.1021/acsestair.4c00015  |
| 546 |  |
| 547 | Conrad BM, Tyner DR, Johnson MR. 2023. Robust probabilities of detection and quantification uncertainty for aerial       |
| 548 | methane detection: Examples for three airborne technologies. Remote Sensing of Environment 288:113499.                   |
| 549 | doi:10.1016/j.rse.2023.113499  |
| 550 |  |
| 551 | Corbett A, Smith B. 2022. A Study of a Miniature TDLAS System Onboard Two Unmanned Aircraft to Independently             |
| 552 | Quantify Methane Emissions from Oil and Gas Production Assets and Other Industrial Emitters. Atmosphere 13:804           |
| 553 | doi:10.3390/atmos13050804  |
| 554 |  |
| 555 | Data portal for carbon Mapper. n.d Carbon Mapper. https://carbonmapper.org/data  |
| 556 |  |
| 557 | Daugėla I, Visockiene JS, Kumpiene J. 2020. Detection and Analysis of Methane Emissions From a Landfill Using            |
| 558 | Unmanned Aerial Drone Systems and Semiconductor Sensors. Detritus 127–138. doi:10.31025/2611-                            |
| 559 | 4135/2020.13942  |

| 560 |  |
|-----|--|
| 561 | Day RE, Emerson E, Bell C, Zimmerle D. 2024. Point Sensor Networks Struggle to Detect and Quantify Short           |
| 562 | Controlled Releases at Oil and Gas Sites. Sensors 24:2419. doi:10.3390/s24082419                                   |
| 563 |  |
| 564 | Erland BM, Adams C, Darlington A, Smith ML, Thorpe AK, Wentworth GR, Conley S, Liggio J, Li S-M, Miller CE,        |
| 565 | Gamon JA. 2022. Comparing airborne algorithms for greenhouse gas flux measurements over the Alberta oil sands.     |
| 566 | Atmospheric Measurement Techniques 15:5841–5859. doi:10.5194/amt-15-5841-2022                                      |
| 567 |  |
| 568 | Foster-Wittig TA, Thoma ED, Green RB, Hater GR, Swan ND, Chanton JP. 2014. Development of a mobile tracer          |
| 569 | correlation method for assessment of air emissions from landfills and other area sources. Atmospheric Environment  |
| 570 | 102:323–330. doi:10.1016/j.atmosenv.2014.12.008  |
| 571 |  |
| 572 | Fredenslund AM, Rees-White TC, Beaven RP, Delre A, Finlayson A, Helmore J, Allen G, Scheutz C. 2018.               |
| 573 | Validation and error assessment of the mobile tracer gas dispersion method for measurement of fugitive emissions   |
| 574 | from area sources. Waste Management 83:68–78. doi:10.1016/j.wasman.2018.10.036                                     |
| 575 |  |
| 576 | Gasbarra D, Toscano P, Famulari D, Finardi S, Di Tommasi P, Zaldei A, Carlucci P, Magliulo E, Gioli B. 2019.       |
| 577 | Locating and quantifying multiple landfills methane emissions using aircraft data. Environmental Pollution         |
| 578 | 254:112987. doi:10.1016/j.envpol.2019.112987   |
| 579 |  |
| 580 | Goldsmith CD, Chanton J, Abichou T, Swan N, Green R, Hater G. 2011. Methane emissions from 20 landfills across     |
| 581 | the United States using vertical radial plume mapping. Journal of the Air & Waste Management Association 62:183-   |
| 582 | 197. doi:10.1080/10473289.2011.639480  |
| 583 |  |
| 584 | Greenhouse Gas Emissions Monitoring. n.d GHGSat. https://www.ghgsat.com/en/  |
| 585 |  |
| 586 | Hollenbeck D, Zulevic D, Chen Y. 2021. Advanced leak detection and quantification of methane emissions using SUAS. |
| 587 | Drones 5:117. doi:10.3390/drones5040117  |
|     |  |

589 Hossain RI, Dudak Y, Buntov P, Canning E, Martino R, Fougère C, Naseridoust S, Bourlon E, Lavoie M, Khaleghi A, 590 Farjami F, Ells L, Berthiaume M-A, Hall C, Risk D. 2024. A controlled release experiment for investigating methane 591 measurement performance at landfills. Environmental Research and Education Foundation. Available from: 592 https://erefdn.org/product/a-controlled-release-experiment-for-investigating-methane-measurement-performance-at-593 landfills/ 594 595 Kahl, J. D., & Chapman, H. L. (2018). Atmospheric stability characterization using the Pasquill method: A critical 596 evaluation. Atmospheric Environment, 187, 196–209. https://doi.org/10.1016/j.atmosenv.2018.05.058 597 598 Kumar, P., Caldow, C., Broquet, G., Shah, A., Laurent, O., Yver-Kwok, C., Ars, S., Defratyka, S., Gichuki, S. W., 599 Lienhardt, L., Lozano, M., Paris, J., Vogel, F., Bouchet, C., Allegrini, E., Kelly, R., Juery, C., & Ciais, P. (2024). 600 Detection and long-term quantification of methane emissions from an active landfill. Atmospheric Measurement 601 Techniques, 17(4), 1229-1250. https://doi.org/10.5194/amt-17-1229-2024 602 603 Ilonze C, Wang J, Ravikumar AP, Zimmerle D. 2024. Methane Quantification Performance of the Quantitative Optical 604 Gas Imaging (QOGI) System Using Single-Blind Controlled Release Assessment. Sensors 24:4044. 605 doi:10.3390/s24134044 606 607 Li HZ, Mundia-Howe M, Reeder MD, Pekney NJ. 2020. Gathering pipeline methane emissions in Utica Shale using 608 an unmanned aerial vehicle and Ground-Based mobile sampling. Atmosphere 11:716. doi:10.3390/atmos11070716 609 610 Mbua M, Riddick SN, Tian S, Cheptonui F, Houlihan C, Smits KM, Zimmerle DJ. 2023. Using controlled subsurface 611 releases to investigate the effect of leak variation on above-ground natural gas detection. Gas Science and Engineering 120:205153. doi:10.1016/j.jgsce.2023.205153 612 613 614 Mchale LE, Martinez B, Miller TW, Yalin AP. 2019. Open-path cavity ring-down methane sensor for mobile monitoring of 615 natural gas emissions. Optics Express 27:20084. doi:10.1364/oe.27.020084 616 MetSens200 - Compact Weather Sensor for Wind with Compass. (n.d.). https://www.campbellsci.com/metsens200 617 MetSens500 - Compact Weather Sensor for Temperature, RH, Barometric Pressure, and Wind with Compass. (n.d.).

| 618 | https://www.campbellsci.com/metsens500   |
|-----|--|
| 619 |  |
| 620 | Mønster J, Kjeldsen P, Scheutz C. 2019. Methodologies for measuring fugitive methane emissions from landfills –    |
| 621 | A review. Waste Management 87:835–859. doi:10.1016/j.wasman.2018.12.047  |
| 622 |  |
| 623 | Morales R, Ravelid J, Vinkovic K, Korbeń P, Tuzson B, Emmenegger L, Chen H, Schmidt M, Humbel S, Brunner D.        |
| 624 | 2022. Controlled-release experiment to investigate uncertainties in UAV-based emission quantification for methane  |
| 625 | point sources. Atmospheric Measurement Techniques 15:2177–2198. doi:10.5194/amt-15-2177-2022                       |
| 626 |  |
| 627 | Mosher BW, Czepiel PM, Harriss RC, Shorter JH, Kolb CE, McManus JB, Allwine E, Lamb BK. 1999. Methane              |
| 628 | emissions at nine landfill sites in the northeastern United States. Environmental Science & Technology 33:2088–    |
| 629 | 2094. doi:10.1021/es981044z  |
| 630 |  |
| 631 | Nisbet EG, Fisher RE, Lowry D, France JL, Allen G, Bakkaloglu S, Broderick TJ, Cain M, Coleman M,                  |
| 632 | Fernandez J, Forster G, Griffiths PT, Iverach CP, Kelly BFJ, Manning MR, Nisbet-Jones PBR, Pyle JA,                |
| 633 | Townsend-Small A, al-Shalaan A, Warwick N, Zazzeri G. 2020. Methane mitigation: methods to reduce                  |
| 634 | emissions, on the path to the Paris Agreement. Reviews of Geophysics 58. doi:10.1029/2019rg000675                  |
| 635 |  |
| 636 | O'Connell E, Risk D, Atherton E, Bourlon E, Fougère C, Baillie J, Lowry D, Johnson J. 2019. Methane emissions      |
| 637 | from contrasting production regions within Alberta, Canada: Implications under incoming federal methane            |
| 638 | regulations. Elementa Science of the Anthropocene 7. doi:10.1525/elementa.341                                      |
| 639 |  |
| 640 | Paris J-D, Riandet A, Bourtsoukidis E, Delmotte M, Berchet A, Williams J, Ernle L, Tadic I, Harder H, Lelieveld J. |
| 641 | 2021. Shipborne measurements of methane and carbon dioxide in the Middle East and Mediterranean areas and the      |
| 642 | contribution from oil and gas emissions. Atmospheric Chemistry and Physics 21:12443–12462. doi:10.5194/acp-21-     |
| 643 | 12443-2021   |
| 644 |  |
| 645 | Ravikumar AP, Sreedhara S, Wang J, Englander J, Roda-Stuart D, Bell C, Zimmerle D, Lyon D, Mogstad I,              |

| 646 | Ratner B, Brandt AR. 2019. Single-blind inter-comparison of methane detection technologies – results from the        |
|-----|--|
| 647 | Stanford/EDF Mobile Monitoring Challenge. Elementa Science of the Anthropocene 7. doi:10.1525/elementa.373           |
| 648 |  |
| 649 | Risk, D., Omidi, A., Bourlon, E., Khaleghi, A., Perrine, G., Tarakki, N., Martino, R., & Stuart, J. (2025, April 3). |
| 650 | Active Face Emissions: an opportunity for reducing methane emissions in global waste management.                     |
| 651 | https://eartharxiv.org/repository/view/8891/   |
| 652 |  |
| 653 | Rutherford J, Sherwin E, Chen Y, Aminfard S, Brandt A. 2023. Evaluating methane emission quantification              |
| 654 | performance and uncertainty of aerial technologies via high-volume single-blind controlled releases. EarthArXiv      |
| 655 | (California Digital Library). doi:10.31223/x5kq0x  |
| 656 |  |
| 657 | Scarpelli TR, Cusworth DH, Duren RM, Kim J, Heckler J, Asner GP, Thoma E, Krause MJ, Heins D, Thorneloe S.           |
| 658 | 2024. Investigating major sources of methane emissions at US landfills. Environmental Science & Technology.          |
| 659 | doi:10.1021/acs.est.4c07572  |
| 660 |  |
| 661 | Sherwin ED, Abbadi SHE, Burdeau PM, Zhang Z, Chen Z, Rutherford JS, Chen Y, Brandt AR. 2024. Single-blind tes        |
| 662 | of nine methane-sensing satellite systems from three continents. Atmospheric Measurement Techniques 17:765–          |
| 663 | 782. doi:10.5194/amt-17-765-2024   |
| 664 |  |
| 665 | Sherwin ED, Chen Y, Ravikumar AP, Brandt AR. 2021. Single-blind test of airplane-based hyperspectral methane         |
| 666 | detection via controlled releases. Elementa Science of the Anthropocene 9. doi:10.1525/elementa.2021.00063           |
| 667 |  |
| 668 | Sherwin ED, Rutherford JS, Chen Y, Aminfard S, Kort EA, Jackson RB, Brandt AR. 2023. Single-blind validation         |
| 669 | of space-based point-source detection and quantification of onshore methane emissions. Scientific Reports 13.        |
| 670 | doi:10.1038/s41598-023-30761-2   |
| 671 |  |
| 672 | Singh D, Barlow B, Hugenholtz C, Funk W, Robinson C, Ravikumar A. 2021. Field Performance of New Methane             |
| 673 | Detection Technologies: Results from the Alberta Methane Field Challenge. EarthArXiv (California Digital             |
| 674 | Library), doi:10.31223/v5gs/6  |

| 675 |   |
|-----|---|
| 676 | Sonderfeld H, Bösch H, Jeanjean APR, Riddick SN, Allen G, Ars S, Davies S, Harris N, Humpage N, Leigh R, Pitt J.    |
| 677 | 2017.Emission estimates from an active landfill site inferred from a combined approach of CFD modelling and in situ |
| 678 | FTIR measurements. Atmospheric Measurement Techniques 10:3931–3946. doi:10.5194/amt-10-3931-2017                    |
| 679 |   |
| 680 | Thorpe AK, O'Handley C, Emmitt GD, DeCola PL, Hopkins FM, Yadav V, Guha A, Newman S, Herner JD, Falk M,             |
| 681 | Duren RM. 2021. Improved methane emission estimates using AVIRIS-NG and an Airborne Doppler Wind Lidar.             |
| 682 | Remote Sensing of Environment 266:112681. doi:10.1016/j.rse.2021.112681   |
| 683 |   |
| 684 | Vermeulen AT, Pieterse G, Hensen A, Van Den Bulk WCM, Erisman JW. 2006. COMET: a Lagrangian transport               |
| 685 | model for greenhouse gas emission estimation – forward model technique and performance for methane. Atmos           |
| 686 | Chem Phys Discuss. doi:10.5194/acpd-6-8727-2006   |
| 687 |   |
| 688 | Wu T, Cheng J, Wang S, He H, Chen G, Xu H, Wu S. 2023. Hotspot Detection and Estimation of Methane                  |
| 689 | Emissions from Landfill Final Cover. Atmosphere 14:1598. doi:10.3390/atmos14111598                                  |
| 690 |   |
| 691 | Yang X, Kuru E, Zhang X, Zhang S, Wang R, Ye J, Yang D, Klemeš JJ, Wang B. 2023. Direct measurement of              |
| 692 | methane emissions from the upstream oil and gas sector: Review of measurement results and technology advances       |
| 693 | (2018–2022). Journal of Cleaner Production 414:137693. doi:10.1016/j.jclepro.2023.137693                            |
| 694 |   |
| 695 | Yong H, Allen G, Mcquilkin J, Ricketts H, Shaw JT. 2024. Lessons learned from a UAV survey and methane              |
| 696 | emissions calculation at a UK landfill. Waste Management 180:47–54. doi:10.1016/j.wasman.2024.03.                   |
| 697 |   |
| 698 |   |
| 699 | Data accessibility statement  |
| 700 | Onsite weather data, release rates and release source location data have been deposited in the Borealis archive:    |
| 701 | https://borealisdata.ca/dataset.xhtml?persistentId=doi:10.5683/SP3/JWF7K2. Although names of participants are not   |

shared, participants are allowed to self-identify. Much of the analysis was completed manually (i.e. using spreadsheets).

Some of the plots were generated using rscripts and they will be added to the dataset.

702

| / UT |  |  |  |
|------|--|--|--|
|      |  |  |  |
|      |  |  |  |
|      |  |  |  |

**Acknowledgments** 

This study was made possible with funding from the Environmental Research and Education Fund and Natural Resources Canada. The authors and contributors acknowledge WM for allowing the use of the Petrolia landfill for this study and for assisting with the regulatory permitting process. The authors thank Augustine van der Baaren and Louise Evans and for editing this manuscript. We thank the contributions of anonymous reviewers whose comments helped to strengthen this report.

711

712

713

704

705

706

707

708

709

710

# Funding information (if applicable)

This study was made possible with funding from the Environmental Research and Education Foundation (EREF).

714

715

## **Author contributions statement**

D. R. conceived the experiment(s). R. H., P. B., Y. D., R. M., C. F., and S. N. conducted the experiment(s). E. B., A. K., and R.H. analyzed the results. R.H wrote the manuscript with assistance from M.L. All authors reviewed the manuscript.

718

719

# **Competing Interests**

- 720 The authors declare no competing interests except to declare their participation in the study as Participants A and N.
- 721 Participants involved in the measurements were prevented from seeing known emission rates until after data
- processing, so we maintain our results are realistic and represent normal outcomes.

| 723<br>724               | Supplementary Material   |           |
|--------------------------|--|-----------|
| 725                      | for  |           |
| 726<br>727<br>728        | A controlled release experiment for investigating methane measurement performance at landfills   |           |
| 729                      | Rafee Iftakhar Hossain <sup>1*</sup> , Pylyp Buntov <sup>1</sup> , Yurii Dudak <sup>1</sup> , Rebecca Martino <sup>1</sup> , Chelsea                 |           |
| 730                      | Fougère <sup>1</sup> , Shadan Naseridoust <sup>2</sup> , Evelise Bourlon <sup>1</sup> , Martin Lavoie <sup>1</sup> , Afshan Khaleghi <sup>2</sup> ,  |           |
| 731                      | Chelsie Hall <sup>1</sup> , and David Risk <sup>1</sup>  |           |
| 732                      | <sup>1</sup> Department of Earth and Environmental Sciences, St Francis Xavier University, Antigonish, Nova Scotia, Canada                           |           |
| 733                      | <sup>2</sup> Faculty of Engineering and Applied Sciences, Memorial University of Newfoundland, St. John's, Newfoundland and                          |           |
| 734                      | Labrador, Canada   |           |
| 735                      | *rhossain@stfx.ca  |           |
| 736<br>737               | Publication in Elementa—Science of the Anthropocene  |           |
| 738                      | Date Sep 19, 2025  |           |
| 739<br>740<br>741<br>742 | Table S1: Minimum detection limits for participants D,J,L and M was reported in kg/hr by participants  | .38<br>on |
| 743                      | Table S3. Dates and times of reported background rates using TruckTC.  |           |
| 744                      | Figure S2. Placement of acetylene tanks during the 2023 controlled release study   | .40       |
| 745                      | Figure S3. Determination of y-intercept value for solution E   | .41       |
| 746                      | Figure S4. Determination of y-intercept values for solution G-2  |           |
| 747                      | Table S4. Y-intercept values for Figures S2 and S3.  |           |
| 748                      | Table S5: Mass flowrates and associated uncertainty of all experiments. Timings are listed in local time (ET)  |           |
| 749                      | Figure S5. Daily wind roses from November 5 to November 10 from the Eastern meteorological station. Station location                                 |           |
| 750                      | are shown in Figure S8.  |           |
| 751<br>752               | Figure S6. Daily wind roses from November 11 to November 14 from the Eastern meteorological station. Stati   |           |
| 752                      | locations are shown in Figure S8Figure S7: Windrose charts of Eastern, Hilltop and Northern Atmospheric Research Stations. Station locations are sho |           |
| 753<br>754               | in Figure S8.  |           |
| 75 <del>4</del><br>755   | Figure S8: Map of controlled release configuration.  |           |
| 756                      | Figure S9: Walking SEM concentration map of the search area  |           |
| 757                      |  |           |
| 758                      |  |           |

## Table of Content:

| 61          | PARTICIPATING SOLUTIONS                                     | <u>30</u> 31             |
|-------------|---|--------------------------|
| 62          | MOBILE TRACER CORRELATION (TRUCKTC)                         | <u>30</u> 32             |
| 63          | AERIAL LIDAR (AIRLIDAR)                                     | <u>31</u> 32             |
| 64          | DRONE COLUMN SENSOR (DRONECS)                               | <u>31</u> 32             |
| 65          | DRONE FLUX PLANE (DRONEFP)                                  | <u>31</u> 32             |
| <b>'</b> 66 | MOBILE GAUSSIAN PLUME (TRUCKGP)                             | <u>32</u> 33             |
| 67          | AIRBORNE POINT SENSOR (AIRFP)                               | <u>32</u> 33             |
| 68          | REMOTE POINT SENSOR(FIXEDPS)                                | <u>32</u> 33             |
| 69          | SATELLITE IMAGING SENSOR (SATME)                            | <u>33</u> 34             |
| 70          | TRUCK LAGRANGIAN (TRUCKLG)                                  | <u>33</u> 34             |
| 71          | BACKGROUND EMISSIONS – RATES AND LOCATIONS                  | 38                       |
| 72          | LOCALIZING BACKGROUND EMISSIONS                             | <u>38</u> 39             |
| 773         | QUANTIFYING BACKGROUND EMISSIONS                            | <u>39</u> 4 <del>0</del> |
| 74          | METHOD 1 – DIRECT TRACER CORRELATION UNDER IDLE CONDITIONS. | <u>39</u> 40             |
| 75          | METHOD 2 – Y-INTERCEPT ANALYSIS DURING ACTIVE RELEASES.     | <u>40</u> 41             |
| 76          | BACKGROUND EMISSIONS - IMPLICATIONS FOR PARTICIPANTS        | <u>42</u> 4 <del>3</del> |
| 77          | BACKGROUND EMISSIONS – SUMMARY                              | <u>42</u> 4 <del>3</del> |
| 78          | FLOW RATES BY EXPERIMENT                                    | <u>43</u> 4 <del>6</del> |
| 79          | WIND AND METEOROLOGICAL CONDITIONS                          | <u>45</u> 48             |
| '80         |   |                          |

## **Participating Solutions**

In the following paragraphs, we provide a brief description of the technical aspects of each method listed in Table 1 under "Method", but we refer the reader to the report by Hossain et al. (2024) for more details. In our descriptions, we use a simplified naming convention where the medium of sensor deployment is mentioned followed by an acronym describing the methodology. We note that some of the methods had dual functions of quantification and detection. Table S1 provides a performance summary for each participant along with operational data collected separately.

## **Mobile Tracer Correlation (TruckTC)**

The Tracer correlation method is the gold standard for quantifying measurements in landfills. This truck-

based method has been used for over two decades (e.g., Mosher et al., 1999), and its errors have been extensively examined (e.g., Fredenslund et al., 2018). The method involves the controlled release of a non-reactive gas, such as acetylene, where tracer gas and methane concentrations are measured downwind and analyzed statistically to establish correlations between the tracer gas and the target gases. In our experiment, the participant performed this tracer release work using a Picarro G2203 dual gas analyzer and worked from the public road system.

#### Aerial LiDAR (AirLiDAR)

Methane detection by AirLiDAR is a widely applied mature solution in the oil and gas sector. Numerous point-source controlled release tests verified that AirLiDAR systems can detect and quantify point source leaks from 1 kg/hr to 3 kg/hr with 90% probability (Bell et al., 2020; Singh et al., 2021; Conrad et al., 2023; Rutherford et al., 2023). Gas mapping AirLiDAR uses a pulsed beam of radiation that reflects off the surface of the ground back to the aircraft where a specialized receiver detects and analyzes the spectral signature of light absorbed or scattered by the methane in the atmosphere.

#### **Drone Column Sensor (DroneCS)**

With the drone Column Sensor (DroneCS), a tunable diode laser is mounted on the underside of an unmanned aerial vehicle (drone) and emits a narrow beam of light at a wavelength appropriate for detecting methane. The energy is bounced off the ground and read by a receiver co-located with the energy source. Measurements are retrieved in ppm\*m. In our study, two participants used Pergam Falcon TDLAS sensors (without gimbal) with flight altitudes of 20 m, a horizontal spacing of 30 m, and 500 ppm\*m threshold values, all of which equated to walking surveys under EPA requirements. DroneCS is a new solution that can potentially supplement or replace walking surveys, but we note that this new technology has not been fully validated.

# **Drone Flux Plane (DroneFP)**

This method uses a drone with a mounted TDLAS, MOS, or other point measurement sensor that has an open cavity or is fed by a small pump. Two participants used DroneFP where the drone flew repeated horizontal transects perpendicular to the wind direction and repeatedly measured at different altitudes to metaphorically paint a screen or curtain. Sometimes called a "flux plane" measurement, the method

senses wind speed, temperature, and pressure values interpolated across the plane, after which the interpolated values are used in a mass balance equation to solve for emission rates. DroneFP is a mature solution and has been validated in point-source controlled release studies at oil and gas sites (Singh et al., 2021; Ravikumar et al., 2019).

# Mobile Gaussian Plume (TruckGP)

In the Mobile Gaussian Plume method (TruckGP), a high-performance methane analyzer is deployed on an on-road vehicle that drives transects through the landfill methane plume, along the downwind fence line, or transects even farther downwind. Wind speed, wind direction, and geo-location are also measured. Emission rates are quantified using a Gaussian dispersion plume model or inversion. A comprehensive study by Fredenslund et al. (2018) found that TruckGP and TruckTC estimates correlated well with R<sup>2</sup> = 0.765. However, Fredenslund et al. (2018) found that TruckGP was more variable and had a predictable low bias where emission rates were normally 72% of the TruckTC estimated rates. Nevertheless, a recent Canadian study showcased TruckGP's utility in screening measurement campaigns (Ars et al., 2020). Our compressed experimental schedule was not ideal for the participants using TruckGP because the timing of releases only allowed about one-fifth of the normal transect replications.

#### Airborne Point Sensor (AirFP)

In the Airborne Point Sensor (AirFP), a high-performance gas analyzer is mounted in an aircraft that flies stacked orbits with radii slightly larger than the site. The first orbit is about 150 m above ground level, and the orbits are repeated at progressively higher altitudes until the aircraft reaches the top of the surface mixed layer. Wind values are measured in the air, or wind estimates are obtained from databases. The low bias could have resulted from the downward extrapolation to the ground (Erland et al., 2022), or from measurements that occurred during highly stable atmospheric conditions when the center of mass for the landfill plumes was below the initial orbit's altitude of 150 m.

#### Remote Point Sensor(FixedPS)

- With the Remote Point Sensor(FixedPS), freestanding stations are located around the landfill perimeter.
- Various environmental sensors measure wind speed, wind direction, temperature, pressure, and

humidity. Methane is detected with a low-cost metal oxide (MOS) sensor or with an open-path Fourier Transform infrared (FT-IR) spectrometer. Algorithms continually estimate emission rates using an inverse source dispersion model, or similar. FixedPS solutions have been scrutinized in oil and gas controlled release studies (Bell et al. 2023, Day et al. 2024) with varying results. The transferability of these oil and gas results to the landfill context is not well understood, and the various FixedPS solutions are still being validated for landfill measurement.

#### **Satellite Imaging Sensor (SatME)**

The Satellite Imaging Sensor (SatME) is a quantification and detection method that incorporates a satellite-mounted sensor that takes a series of images and collects methane column measurements for individual pixels. Quantification is by Integrated Mass Enhancement Method. Generally, SatME easily detects large point source emissions within a facility, whereas area-based sources could be missed because the plumes lack opacity at target wavelengths. Several studies have validated SatME as a way to detect and quantify point source emissions with good results at high emission rates. Sherwin et al. (2023) found that the most sensitive current satellites can detect a point source emission as small as 170 kg/hr, although the expected detection success would vary for area sources.

#### Truck Lagrangian (TruckLG)

This method combines the same type of truck-based sampling used in TruckGP with a prototypical Lagrangian post-processing algorithm applicable at landfill scales. Lagrangian models are commonly used to predict source location probabilities and can be used to calculate emission rates, normally from tower measurements, for point- or area-based sources. Vermeulen et al. (2006) used the City-based Optimization Model for Energy Technologies (COMET) model to simulate GHG concentrations in the Netherlands and Ireland, and Paris et al. (2021) assessed methane emissions from offshore oil platforms in the Norwegian Sea using a Lagrangian model. However, our experimental schedule was not ideal for the participants using TruckLG, because the timing of the releases only permitted a fraction of the normal transect replications.

| Technology<br>Identifier | Method  | R&D? | Cost   | Comments  | Vendor<br>Reported<br>minimum<br>detection<br>limit |
|--------------------------|---------|------|--------|---|---|
| A                        | TruckGP | No   | Low    | Reported approximately 66% of known release rates with a tendency to underestimate emission rates. Method is usually deployed over several hours and short release windows affected quantification performance. Method offered flexibility and extended duty cycle across weather conditions and was able to report measurements on each day of the experiment. | 5 kg/hr   |
| В                        | TruckGP | No   | Low    | Reported approximately 56% of known release rates with a tendency to underestimate emission rates. Method is usually deployed over several hours and short release windows affected quantification performance. Method offered flexibility and extended duty cycle across weather conditions and was able to report measurements on each day of the experiment. | 5 kg/hr   |
| C                        | DroneFP | No   | Medium | Quantification estimates were very good with few outliers. Methodology is affected by weather conditions where measurements are not possible during rain and windspeed above 12 m/s. During localization trials, methodology did not register any true positive emission estimates during the localization phase of the study.                                  | 0.02 kg/hr  |
| D                        | DroneFP | No   | Medium | Estimates varied greatly from true release rates with bias being less predictable. Methodology is affected by weather conditions where measurements are not possible during precipitation and windspeed above 17 m/s.   | 1 ppb/s   |
| E                        | TruckTC | No   | Medium | Quantification estimates were consistently close to true release rates with a slight downward bias. Method requires setup of tracer gas and frequent monitoring of its consumption levels. Method offered flexibility and extended duty cycle across weather conditions and was able to report measurements on each day of the experiment.                      | 5 kg/hr   |

| F | AirFP    | No  | High   | Underestimated measurements consistently and vendor reported that estimates were not classified as high quality due to internal meteorological for measurements were not met. Requires 2-6 m/s windspeed, solar insolation and not a lot of cloud cover for good   | 3-5 kg/hr                |
|---|----------|-----|--------|--|--------------------------|
| G | AirLiDAR | No  | High   | measurements.  Both LiDAR and mass balance methods were accurate and had a tendency to overestimate emission rates. Increase in quantification estimates were observed after onsite weather data were considered. Requires good visual flight rules conditions for flying aircraft. Ideal wind speed ranges from 3- 6 m/s.  Performed very well detecting active | 0.5 kg/hr                |
|   |          |     |        | emissions 100 percent of the time without false positive readings.   |                          |
| Н | SatME    | No  | Medium | Emissions were not detected for quantification or localization purposes. Minimum detection limit expected to be at least 300 kg/hr. Cloud cover over the site and/or wind speed exceeding 10 m/s prevents emission measurement.  | 100 kg/hr                |
| I | FixedPS  | Yes | Medium | Overestimated emissions in most cases. Low maintenance method of quantifying estimates, due to low number of sensors only a limited set of wind conditions were covered.   | Not<br>available         |
| J | FixedPS  | Yes | Medium | Provided the closest measurements to actual emission values compared to other fixed sensors. Due to low number of sensors only a limited set of wind conditions were covered.  | 100 ppm at<br>100 meters |
| K | FixedPS  | Yes | Medium | Underestimated emission in most cases. Due to low number of sensors only a limited set of wind conditions were covered.  | 1 kg/hr                  |
| L | DroneCS  | No  | Medium | Reported high number of false positive estimates with limited visibility when measuring active emission points on slopes. Minimum detection limit at 90 % probability of detection was determined to be 95.34 kg/hr. Methodology is affected by weather conditions where measurements are not possible during rain and windspeed above 12 m/s.                   | 1 ppm                    |

| M | DroneCS | No  | Medium | Performed slightly better than compared to other methods using TDLAS sensors. Also had high number of false positives and a minimum detection limit at 90% probability of detection of 101.88 kg/hr. Methodology is affected by weather conditions where measurements are not possible during rain and windspeed above 12 m/s. | 1 ppm   |
|---|---------|-----|--------|--|---------|
| N | TruckLG | Yes | Low    | Overestimated emissions in most cases. Lagrangian models are usually applied to tower-based systems however in this instance it was adapted to a mobile setting.   | 5 kg/hr |

Table S1: Minimum detection limits for participants D,J,L and M was reported in kg/hr by participants.

| Participant  | Number Experiment Participated | Number Experiment Reported |
|--------------|--------------------------------|----------------------------|
| A (TruckGP)  | 35                             | 30                         |
| B (TruckGP)  | 41                             | 31                         |
| C (DroneFP)  | 16                             | 15                         |
| D (DroneFP)  | 9                              | 6                          |
| E (TruckTC)  | 36                             | 28                         |
| F (AirFP)    | 10                             | 10                         |
| G (AirLiDAR) | 13                             | 13                         |
| H (SatME)    | 5                              | N/A                        |
| I (FixedPS)  | R&D                            | 17                         |
| J (FixedPS)  | R&D                            | 25                         |

| K (FixedPS) | R&D | 31 |
|-------------|-----|----|
| L (DroneCS) | 6   | 6  |
| M (DroneCS) | 7   | 4  |
| N (TruckLG) | R&D | 10 |

Table S2: Number of experiments measured vs. reported; R&D unscheduled, Participant G had no detections.

#### **Background Emissions - Rates and Locations**

The controlled release site was a closed landfill chosen because it replicates landfill-scale topography and emissions complexity while maintaining unusually low residual methane fluxes. Its cap system is atypically robust: geotextile plus clay overlain by >1.5 m of soil, with an active vertical well collection system operating at negative pressure. This configuration achieves rare 98–99% gas collection efficiency, verified by comparing background fluxes against collected gas burned for electricity generation—performance seldom matched by North American landfills. While natural landforms such as drumlins might have eliminated residual emissions altogether, finding one of appropriate scale, slope, vegetation cover, and proximity to gas delivery was impractical. Accepting modest background emissions was a deliberate tradeoff to achieve otherwise optimal site attributes.

# **Localizing Background Emissions**

Background sources are spatially distinct from the 20-acre experimental "search area," which we surveyed with EPA Method 21 walking methods. Within this area, near-surface concentrations (5–10 cm) were atmospheric, with only rare localized enhancements of 0.1–0.2 ppm. Thus, participants working within or at the perimeter of the search area encountered negligible background influence.

Confounding sources were located primarily along broader landfill site boundaries. Using a combination of LiDAR and EPA Method 21 walking surveys, and incorporating information of various types communicated to us by several measurement vendors, we identified ~11 discrete emission points (Figure S2). Ten were onsite, distributed along the northwest, west, south, and southeast boundaries, each typically 1–3 kg h<sup>-1</sup>. A larger source lay offsite by about 500 m to the northeast but is not considered in our estimate of background emissions for the landfill since it represents an offsite source originating from different activities and owners. Offsite sources are normal interferents for measurement technologies applied beyond fenceline, and could have affected results when measurement teams were directly downwind – although measurement teams did not communicate to us how or whether they adjusted for the offsite source. All measurement teams were advised of the offsite source presence. The landfill background emission sources were mainly manholes venting the leachate system, but also the onsite electricity generation facility burning collected landfill gas, and a localized cover leak. Rates and exact coordinates are withheld to preserve blindness for future studies.



Figure S2.Confounding sources (blue) and search area (white); identified via LiDAR, quantified by tracer correlation.

#### 

#### **Quantifying Background Emissions**

We applied two independent approaches to quantify background methane emissions.

#### Method 1 - Direct tracer correlation under idle conditions.

Truck-based Tracer Correlation (TruckTC) measurements were conducted repeatedly when the release system was idle, yielding a mean background flux of 24.4 kg h<sup>-1</sup> with a standard deviation of 8.8 kg h<sup>-1</sup> (Table S3). This is a direct measurement of prevailing background conditions, and values were added to release rates when adjudicating offsite participant results.

| Date       | Start        | End          | Release Rate [kg/hr] |
|------------|--------------|--------------|----------------------|
| 2023-11-07 | 09:07:14.204 | 09:23:32.305 | 19                   |
| 2023-11-07 | 09:21:02.026 | 09:28:01.880 | 34                   |

| 2023-11-07 | 09:25:27.328 | 09:34:35.483 | 12 |
|------------|--------------|--------------|----|
| 2023-11-07 | 09:30:31.747 | 09:37:09.141 | 42 |
| 2023-11-07 | 16:18:11.186 | 16:18:37.052 | 24 |
| 2023-11-07 | 16:20:26.043 | 16:21:22.318 | 25 |
| 2023-11-07 | 16:23:59.127 | 16:25:03.404 | 24 |
| 2023-11-08 | 08:19:06.463 | 08:19:34.638 | 23 |
| 2023-11-09 | 08:07:31.650 | 08:09:30.875 | 17 |

Table S3. Dates and times of reported background rates using TruckTC.



Figure S2. Placement of acetylene tanks during the 2023 controlled release study.

#### Method 2 - Y-intercept analysis during active releases.

For two high-performing offsite systems—TruckTC and Flux-Plane AirLiDAR G-2—we examined the y-intercept of linear regression fits between measured and released fluxes (Figures S2–S3) during active release conditions and without adding or correcting for background emissions. We included TruckTC and LiDAR because they incorporated: (a) true offsite operation (fenceline or beyond), (b) high accuracy and low residuals, and (c) strong correlation ( $R^2 > 0.75$ ) between measured and released fluxes in the release experiments. The resulting y-intercepts (19.4 and 22.0 kg  $h^{-1}$ ; mean  $\approx 20.7$  kg  $h^{-1}$ ) indicate the background release rate, and closely matched direct TruckTC idle measurements (Table S4), confirming consistency between independent methods.

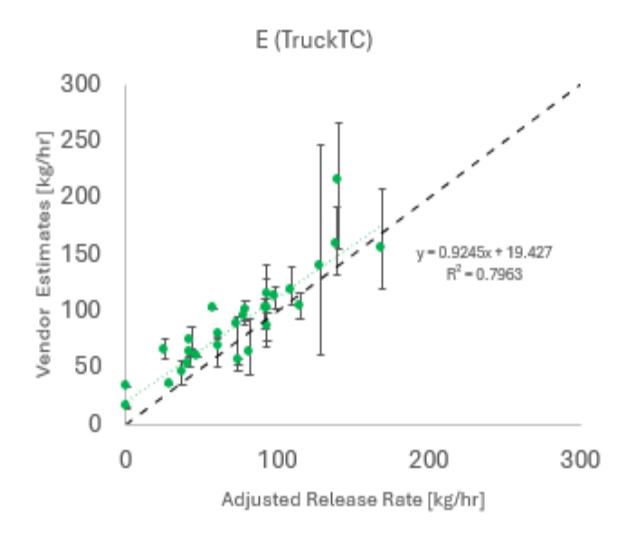


Figure S3. Determination of y-intercept value for solution E.

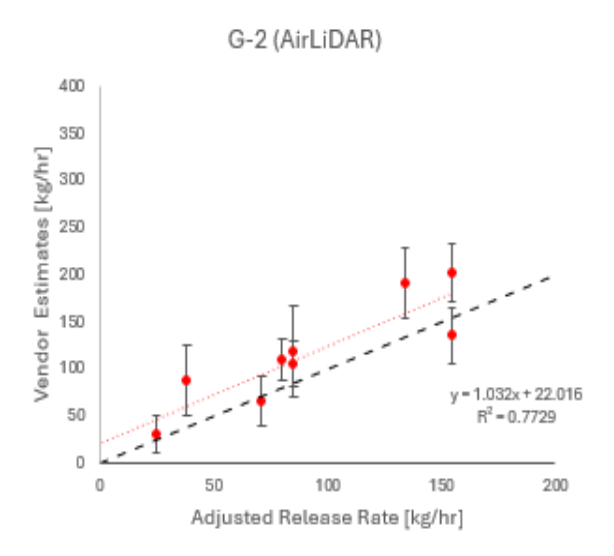


Figure S4. Determination of y-intercept values for solution G-2.

| Solution                     | n  | R <sup>2</sup> | intercept |
|------------------------------|----|----------------|-----------|
| E (Truck TC) S2              | 27 | 0.80           | 19.43     |
| G-1 (AirLiDAR Flux Plane) S3 | 9  | 0.77           | 22.02     |
|                              |    | mean:          | 20.725    |

Table S4. Y-intercept values for Figures S2 and S3.

Together, these two independent approaches constrain background emissions to ~20–25 kg h<sup>-1</sup>, with variability that is normally distributed and therefore unlikely to bias participant results, though it does increase scatter.

#### **Background Emissions - Implications for Participants**

For the minority of participants whose sensing path crossed background sources (e.g., roadside or distal deployments), background emissions were included in adjudications and shown in parity plots via x-axis error bars representing the standard deviation of Method 1 estimates. However, most participants reported measurement uncertainties much larger than the background variability, rendering its contribution negligible. Indeed, terrain, wind shear, coincident multi-source plumes, and other real-world complexities proved to be more important determinants of performance. Only the most accurate systems, those already demonstrating tight agreement with controlled releases, could plausibly have had their outcomes shifted by the ~20 kg h<sup>-1</sup> background. For others, methodological challenges dominated.

#### **Background Emissions - Summary**

In sum, background emissions were modest, well-constrained by two independent methods, and treated transparently in our analysis. They represent a small tradeoff for the realism and scale afforded by this unique landfill site. Their effect was primarily to increase data scatter, with negligible impact on most participant outcomes. Only the highest-performing technologies approached the precision where background variability might influence adjudication, underscoring that broader methodological improvements remain the priority for most teams.

### 1020 Flow Rates by Experiment

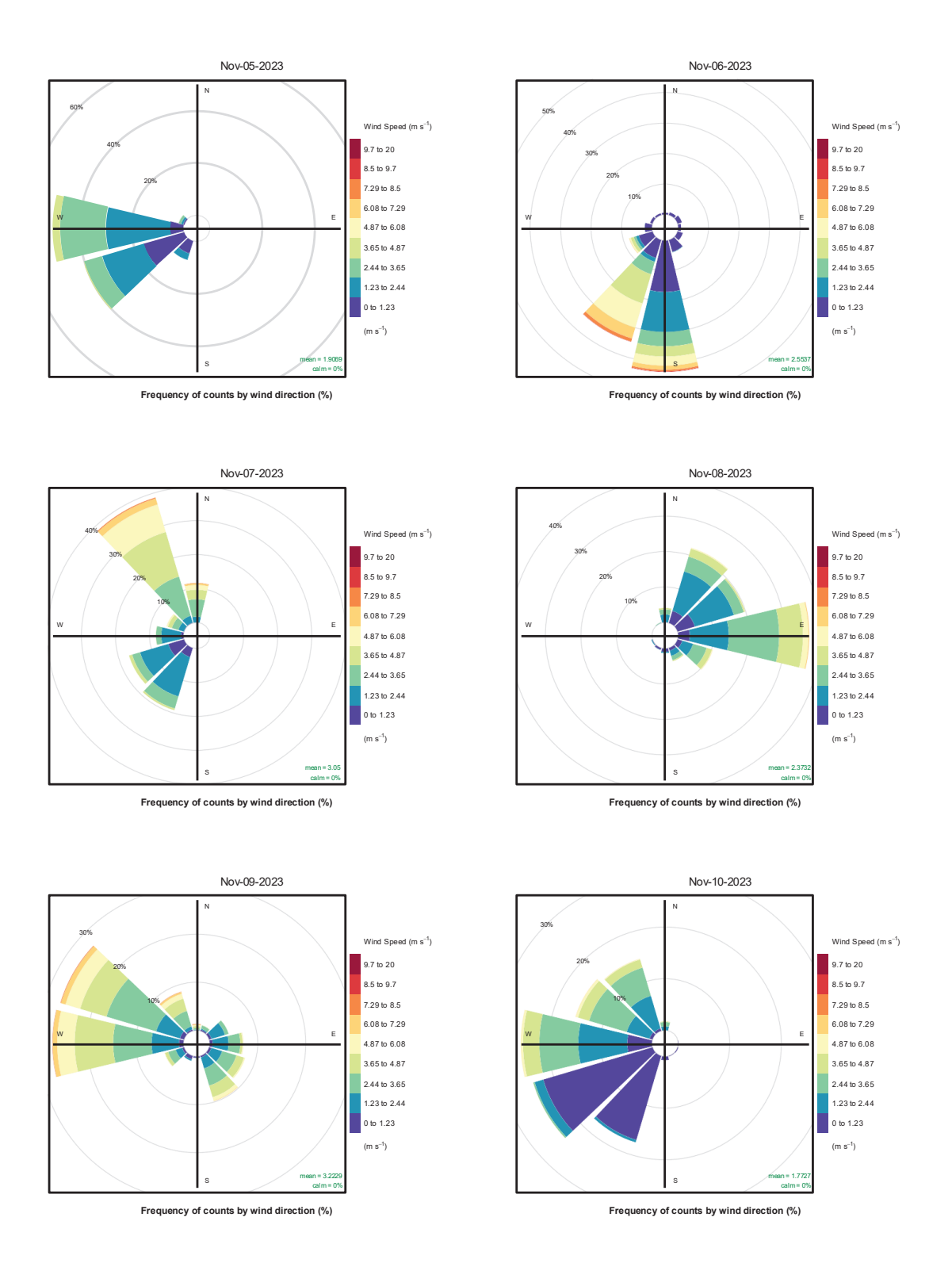
| Fig.    | Flov     | w R           | ates     | s by | Exp | peri | mer      | ıt      |         |    |          |       |          |                      |                      |    |    |    |          |          |          |         |         |          |          |      |            |
|--|----------|---------------|----------|------|-----|------|----------|---------|---------|----|----------|-------|----------|----------------------|----------------------|----|----|----|----------|----------|----------|---------|---------|----------|----------|------|------------|
| 1  | Ex<br>p# |               |          |      |     |      | Q_<br>D3 | Q_<br>E | Q_<br>F |    | Q_<br>K5 | meter | e<br>Tot |                      |                      |    |    |    | Q_<br>D1 | Q_<br>D2 | Q_<br>D3 | Q_<br>E | Q_<br>F | Q_<br>K4 | Q_<br>K5 | RSS  | %U         |
| 2  | 1        |               |          |      |     |      |          |         |         |    |          | 19.49 | 43.      | 06T10:00             | 06T10:40             |    |    |    | 0        | 0        |          |         |         | 0        | 0        |      | 0.0<br>108 |
| 1  | 2        |               |          |      |     |      |          |         |         |    |          | 28.50 |          | 2023-11-<br>06T11:40 | 2023-11-<br>06T12:20 |    |    |    |          | 0        | 0        |         |         | 0        |          |      | 0.0<br>126 |
| 1  | 3        | 0.0           |          |      |     |      |          |         |         |    |          | 0.30  |          | 2023-11-<br>06T12:40 | 2023-11-<br>06T13:30 | 0  | 0  |    |          | 0        | 0        |         |         |          | 0        |      | 0.0<br>09  |
| Section   Column    | 4        |               |          |      |     |      |          |         |         |    |          | 82.03 |          | 2023-11-<br>06T13:53 | 2023-11-<br>06T14:43 |    |    |    | 0        |          | 0        |         |         |          | 0        |      | 0.0<br>126 |
| Column   C | 5        |               |          |      |     |      |          |         |         |    |          | 74.04 |          | 2023-11-<br>06T15:41 | 2023-11-<br>06T16:30 |    | 0  |    | 0        |          | 0        |         |         | 0        |          |      | 0.0<br>108 |
|  | 6        |               |          |      |     |      |          |         |         |    |          | 28.44 |          | 07T08:16             | 07T09:06             |    |    |    | 0        | 0        |          |         |         |          | 0        |      | 0.0<br>126 |
|  | 7        |               |          |      |     |      |          |         |         |    |          | 25.53 |          | 07T09:40             | 2023-11-<br>07T10:30 | 0  | 0  | 0  | 0        | 0        | 0        |         |         |          | 0        |      | 0.0<br>054 |
| B  | 8        | -<br>0.0<br>1 | 0.0<br>1 |      |     |      |          |         |         |    |          | 0.25  | 68       | 07T11:11             | 07T12:10             | 0  | 0  |    | 0        | 0        | 0        | 0       |         |          | 0        |      | 0.0<br>054 |
| 4  | 9        |               |          |      |     |      |          |         |         |    |          | 98.87 |          | 07T12:30             | 07T13:20             |    |    |    |          | 0        | 0        |         |         | 0        |          |      | 0.0<br>126 |
| Description   Property   Proper |          |               | 2        | 11   | 19  |      | 0        | 71      | 47      |    | 4        | 8     | .42      | 07T13:40<br>:15.331  | 07T14:30<br>:28.162  | 06 | 06 | 06 |          |          |          | 06      |         |          | 06       | 0126 | 0.0<br>126 |
| 1  |          | 0             | 8        | 6    | 0   | 5    | 0        | 92      | 74      | 6  | 0        |       | 94       | 07T14:45<br>:05.445  | 07T15:18<br>:11.408  | 06 | 06 | 06 |          | 06       |          | 06      | 06      | 06       |          | 0126 | 0.0<br>126 |
| D  |          |               |          |      |     |      |          |         |         | 1  | 0        |       | 97       | 07T15:26<br>:14.286  | 07T15:56<br>:16.816  |    |    |    | 0        |          | 0        | 06      |         |          |          | 0126 | 0.0<br>126 |
| 14   |          | 0             | 1        | 0    | 0   | 0    | 0        | 78      | 16      | 4  | 0        |       | .40      | 08T08:13<br>:40.905  | 08T09:04<br>:52.638  | 06 |    |    |          |          |          | 06      | 06      | 06       |          | 0072 | 0.0<br>072 |
| No.   14   3   0   0   8   13   04   8   0   0   24   06110:17   70   06   06   06   06   06   06   0  |          | 14            | 1        | 3    | 1   | 0    | 0        | 94      | 55      | 0  | 7        | 4     | .18      | 08T09:17<br>:03.823  | 08T10:07<br>:27.289  | 06 | 06 | 06 | 06       |          |          | 06      | 06      |          | 06       | 0126 | 0.0<br>126 |
| 56   56   56   56   50   0   55   6.1   2   56   0   41   0671150   0718241   0   06   06   0   0   0   0   0   0  |          | 0             | 14       | 3    | 0   | 0    | 8        |         | 04      | 8  | 0        | 0     | .24      | 08T10:17<br>:27.030  | 08T11:07<br>:27.828  | 06 | 06 | 06 |          |          | 06       | 06      | 06      | 06       |          | 0126 | 0.0<br>126 |
| 99   56   71   0   37   0   32   87   85   0   7   .11   .08712.55   08713.45   08   08   06   06   06   06   06   06  |          | 56            | 56       | 56   | 0   | 0    | 55       | 5       | 2       | 56 | 0        |       | .41      | 08T11:50<br>:14.469  | 08T12:40<br>:19.682  | 06 | 06 | 06 |          |          | 06       |         | 06      | 06       |          | 0108 | 0.0<br>108 |
| 1  |          | 99            |          | 71   | 0   | 37   | 0        | 32      | 87      | 85 | 0        | 7     | .11      | 08T12:55<br>:33.269  | 08T13:45<br>:37.403  | 06 | 06 | 06 |          | 06       |          | 06      | 06      | 06       |          | 0126 | 0.0<br>126 |
| 0 1 0 0 0 0 0 0 0 0 0 0 43 70 9 0 0 24 09T0845 09T0820 06 06 06 06 06 06 06 06 06 06 06 06 06  |          | 0             | 0.0<br>1 | 0    | 0   | 0    | 0        | 75      | 70      | 8  | 0        |       | .56      | 09T08:00<br>:22.677  | 09T08:45<br>:00.432  |    |    | 06 |          |          |          | 06      | 06      | 06       |          | 0072 | 0.0<br>072 |
| 0.0   3   6   8   0   0   49   71   7   0   66   60   60   60   60   60  |          |               | 1        | 0    | 0   | 0    | 0        | 43      | 70      | 9  | 0        |       | .24      | 09T08:45<br>:02.120  | 09T09:20<br>:31.461  |    |    | 06 | 06       |          |          | 06      | 06      | 06       |          | 009  | 0.0        |
| 0.0  |          | 1             | 3        | 6    | 8   | 0    | 0        | 49      | 71      | 7  | 0        |       | 66       | 09T09:30<br>:17.935  | 09T10:15<br>:03.745  |    | 06 | 06 | 06       |          |          | 06      | 06      | 06       |          | 0108 | 0.0<br>108 |
| 0.0  |          |               | 3        | 6    | 8   | 0    | 0        |         | 70      | 3  | 0        |       | 62       | 09T10:15<br>:05.662  | 09T10:45<br>:20.562  |    | 06 | 06 | 06       |          |          | 06      | 06      | 06       |          | 0108 | 0.0<br>108 |
| 0.0  |          |               | 0        | 0    | 0   | 0    | 0        | 4       | 8       | 3  | 0        |       | 80       | 09T11:00<br>:02.155  | 09T11:30<br>:00.364  |    |    | 06 | 06       |          |          |         | 06      | 06       |          | 0072 | 0.0<br>072 |
| 0.0  |          |               | 56       | 8    | 0   | 71   | 0        | 20      | 20      | 0  | 56       | 0     | .94      | 09T11:35<br>:15.208  | 09T12:05<br>:16.021  | _  | 06 | 06 |          | 06       | 0        | 06      | 06      |          | 06       | 0108 | 108        |
| 56   56   8   4   0   0   0   0   0   2   0   8   07   09T12-45   09T13-15   06   06   06   06   06   06   06   0  |          | 1             | 0        | 0    | 0   | 0    | 0        |         | 20      | 5  | 0        |       | 16       | 09T12:09<br>:59.947  | 09T12:40<br>:08.841  |    |    | 06 | 06       |          | 0        | 06      | 06      | 06       | _        | 009  | 09         |
| 56   56   8  |          | 56            | 56       | 8    | 4   | 0    | 0        | 1       | 2       | 0  | 8        |       | 07       | 09T12:45<br>:14.837  | 09T13:15<br>:21.213  | 06 | 06 | 06 | 06       |          |          |         | 06      |          | 06       | 0108 | 108        |
| The color of the |          | 56            | 56       | 8    | 4   | 0    | 0        | 6       | 0       | 0  | 7        |       | 12       | 09T13:20<br>:08.104  | 09T13:50<br>:16.090  | 06 | 06 | 06 | 06       |          |          | 06      | 06      |          | 06       | 0126 | 0.0<br>126 |
| 0.0   0   5   0   0   8   49   70   9   0   55   09T15:10   09T15:40   06   06   06   06   06   06   099   05  |          |               | 5        | 14   | 0   | 0    | 8        | 77      | 44      | 4  | 0        | 9     | .62      | 09T14:20<br>:39.444  | 09T15:00<br>:40.360  | 06 | 06 | 06 |          |          | 06       | 06      | 06      | 06       |          | 0126 | 126        |
| 56   56   56   0   0   56   0   0   56   0   0   2   56   0   0   .51   09T16:50   09T16:30   06   06   06   06   06   06   06   |          | 1             | 0        | 5    | 0   | 0    | 8        |         | 70      | 9  | 0        |       | 55       | 09T15:10<br>:07.250  | 09T15:40<br>:11.989  |    |    | 06 |          |          | 06       | 06      | 06      | 06       |          | 009  | 0.0<br>09  |
| 7 92 8 0 1 0 33 11 0 8 15 09T16:50 09T17:30 06 06 06 06 06 06 06 06 06 06 06 06 06   |          | 56            | 56       | 56   | 0   | 0    | 56       | 6       | 2       | 56 | 0        |       | .51      | 09T15:50<br>:00.857  | 09T16:30<br>:06.796  | 06 | 06 | 06 |          |          | 06       |         | 06      | 06       |          | 0108 | 108        |
| 0 0.0 0 0 0 0 0 0 0 0 0 0 0 0 0 0 0 0 0  |          | 7             |          | 8    | 0   | 1    | 0        | 33      | 11      | 0  | 8        |       | .15      | 09T16:50<br>:02.293  | 09T17:30<br>:04.556  | 06 | 06 | 06 |          | 06       |          | 06      | 06      |          | 06       | 0126 | 126        |
| 56 56 56 56 0 0 0 0.1 2 56 0 0 .46 10T08:49 10T09:19 06 06 06 06 06 06 06 06 06 06 06 06 06  |          | 0             | 1        | 0    | 0   | 0    | 0        |         | 09      | 3  | 0        |       | 61       | 10T08:09<br>:19.152  | 10T08:39<br>:30.471  |    |    | 06 |          |          |          | 06      | 06      | 06       |          | 0072 | 0.0<br>072 |
| , oo , o.o , - , o.o , o.o , o.o , o.o , io. , io. , io. , o.o , o.o , or. or , or , ii- , 2025-ii- , 0 , 0 , 0 , 0 , 0 , 0 , 0 , 0 , 0 ,  |          | 56            | 56       | 56   | 56  | 0    | 0        | 0       | 2       | 56 | 0        |       | .46      | 10T08:49<br>:00.098  | 10T09:19<br>:03.130  | 06 | 06 | 06 | 06       |          |          |         | 06      | 06       |          | 0108 | 0.0<br>108 |
| 0 0.0 0 0 0 0 54 55 0 0 0 52 10T09:59 06 06 06 06 06 06 009 09   | 33       |               | 0.0      |      |     |      |          |         |         |    |          | 31.06 |          | 10T09:29             | 10T09:59             | U  | U  |    |          | U        | U        |         |         |          | Ü        |      | 0.0<br>09  |

| Ex<br>p# | Q_<br>A   | Q_<br>B       | Q_<br>C   | Q_<br>D1  | Q_<br>D2  | Q_<br>D3  | Q_<br>E   | Q_<br>F   | Q_<br>K4  | Q_<br>K5  | Flow<br>meter<br>Total | Sit<br>e<br>Tot | Time<br>Start                              | Time<br>End                                | U_<br>A   | U_<br>B   | C_        | Q_<br>D1  | Q_<br>D2  | Q_<br>D3  | Q_<br>E   | Q_<br>F   | Q_<br>K4  | Q_<br>K5  | RSS          | %U         |
|----------|-----------|---------------|-----------|-----------|-----------|-----------|-----------|-----------|-----------|-----------|------------------------|-----------------|--|--|-----------|-----------|-----------|-----------|-----------|-----------|-----------|-----------|-----------|-----------|--------------|------------|
| 34       | 16.<br>51 | 16.<br>54     | 16.<br>51 | 16.<br>21 | 0.0       | 0.0       | 0.0       | 0.0       | 0.0       | 15.<br>59 | 81.35                  | 105<br>.79      | 2023-11-<br>10T10:10                       | 2023-11-<br>10T10:53                       | 0.0<br>06 | 0.0<br>06 | 0.0<br>06 | 0.0<br>06 | 0         | 0         | 0         | 0.0<br>06 | 0         | 0.0<br>06 | 0.00<br>0108 | 0.0<br>108 |
| 35       | 4.6<br>4  | 4.6<br>4      | 0.0       | 0.0       | 0.0       | 0.0       | 4.6       | 4.6<br>4  | 4.6<br>4  | 0.0       | 23.19                  | 47.<br>63       | :01.056<br>2023-11-<br>10T11:02<br>:06.039 | :17.864<br>2023-11-<br>10T11:32<br>:05.908 | 0.0<br>06 | 0.0<br>06 | 0.0<br>06 | 0         | 0.0<br>06 | 0         | 0.0<br>06 | 0.0<br>06 | 0.0<br>06 | 0         | 0.00<br>0126 | 0.0<br>126 |
| 36       | 0.0       | 0.0           | 0.0       | 0.0       | 0.0       | 0.0       | 27.<br>84 | 27.<br>84 | 0.0       | 0.0       | 55.69                  | 80.<br>13       | 2023-11-<br>10T12:30<br>:00.096            | 2023-11-<br>10T13:10<br>:06.739            | 0         | 0.0<br>06 | 0.0<br>06 | 0.0<br>06 | 0         | 0         | 0.0<br>06 | 0.0<br>06 | 0.0<br>06 | 0         | 0.00<br>0108 | 0.0<br>108 |
| 37       | 18.<br>56 | 18.<br>56     | 18.<br>56 | 18.<br>56 | 0.0       | 0.0       | 18.<br>55 | 18.<br>56 | 18.<br>56 | 0.0       | 129.9<br>2             | 154<br>.36      | 2023-11-<br>10T13:15<br>:08.208            | 2023-11-<br>10T13:55<br>:03.609            | 0.0<br>06 | 0.0<br>06 | 0.0<br>06 | 0.0<br>06 | 0         | 0         | 0.0<br>06 | 0.0<br>06 | 0.0<br>06 | 0         | 0.00<br>0126 | 0.0<br>126 |
| 38       | 18.<br>56 | 18.<br>56     | 18.<br>56 | 0.0       | 0.0       | 18.<br>56 | 18.<br>56 | 18.<br>56 | 0.0       | 18.<br>56 | 129.9<br>4             | 154<br>.38      | 2023-11-<br>10T14:00<br>:12.192            | 2023-11-<br>10T14:40<br>:13.075            | 0.0<br>06 | 0.0<br>06 | 0.0<br>06 | 0         | 0         | 0.0<br>06 | 0.0<br>06 | 0.0<br>06 | 0         | 0.0<br>06 | 0.00<br>0126 | 0.0<br>126 |
| 39       | 0.0       | -<br>0.0<br>1 | 0.0       | 6.5<br>0  | 0.0       | 0.0       | 19.<br>49 | 16.<br>70 | 0.0       | 0.0       | 42.69                  | 67.<br>13       | 2023-11-<br>10T15:05<br>:01.397            | 2023-11-<br>10T15:35<br>:06.503            | 0         | 0         | 0.0<br>06 | 0.0<br>06 | 0         | 0         | 0.0<br>06 | 0.0<br>06 | 0.0<br>06 | 0         | 0.00<br>009  | 0.0<br>09  |
| 40       | 9.2<br>8  | 9.2<br>8      | 0.0       | 0.0       | 0.0       | 0.0       | 0.0       | 0.0       | 9.2<br>8  | 0.0       | 27.86                  | 52.<br>30       | 2023-11-<br>10T15:40<br>:00.740            | 2023-11-<br>10T16:10<br>:06.764            | 0.0<br>06 | 0.0<br>06 | 0.0<br>06 | 0         | 0.0<br>06 | 0         | 0.0<br>06 | 0.0<br>06 | 0.0<br>06 | 0         | 0.00<br>0126 | 0.0<br>126 |
| 41       | 18.<br>56 | 18.<br>56     | 18.<br>56 | 0.0       | 18.<br>49 | 0.0       | 27.<br>83 | 27.<br>84 | 18.<br>56 | 0.0       | 148.4<br>2             | 172<br>.86      | 2023-11-<br>10T16:15<br>:19.908            | 2023-11-<br>10T16:45<br>:20.823            | 0.0<br>06 | 0.0<br>06 | 0.0<br>06 | 0         | 0.0<br>06 | 0         | 0.0<br>06 | 0.0<br>06 | 0.0<br>06 | 0         | 0.00<br>0126 | 0.0<br>126 |
| 42       | 18.<br>56 | 0.0           | 0.0       | 18.<br>56 | 0.0       | 0.0       | 50.<br>22 | 0.0       | 0.0       | 0.0       | 87.36                  | 111<br>.80      | 2023-11-<br>11T09:51<br>:39.948            | 2023-11-<br>11T10:50<br>:10.126            | 0.0<br>06 | 0.0<br>06 | 0.0<br>06 | 0.0<br>06 | 0         | 0         | 0.0<br>06 | 0.0<br>06 | 0         | 0.0<br>06 | 0.00<br>0126 | 0.0<br>126 |
| 43       | 0.0       | 18.<br>56     | 18.<br>56 | 0.0<br>0  | 0.0       | 0.0       | 9.2<br>7  | 55.<br>68 | 0.0       | 0.0       | 102.0<br>8             | 126<br>.52      | 2023-11-<br>11T11:00<br>:08.579            | 2023-11-<br>11T12:00<br>:12.439            | 0         | 0.0<br>06 | 0.0<br>06 | 0         | 0.0<br>06 | 0         | 0.0<br>06 | 0.0<br>06 | 0.0<br>06 | 0         | 0.00<br>0108 | 0.0<br>108 |
| 44       | 0.0       | 0.0           | 0.0       | 0.0       | 0.0       | 0.0       | 0.0       | 9.2<br>8  | 0.0       | 0.0       | 9.28                   | 33.<br>72       | 2023-11-<br>11T12:10<br>:19.641            | 2023-11-<br>11T12:40<br>:27.410            | 0         | 0.0<br>06 | 0.0<br>06 | 0.0<br>06 | 0         | 0         | 0.0<br>06 | 0.0<br>06 | 0         | 0.0<br>06 | 0.00<br>0108 | 0.0<br>108 |
| 45       | 0.0       | 0.0           | 0.0       | 0.0       | 4.6<br>4  | 0.0       | 9.2<br>4  | 0.0       | 0.0       | 0.0       | 13.89                  | 38.<br>33       | 2023-11-<br>11T13:02<br>:55.106            | 2023-11-<br>11T13:28<br>:55.765            | 0         | 0         | 0.0<br>06 | 0         | 0.0<br>06 | 0         | 0.0<br>06 | 0.0<br>06 | 0         | 0         | 0.00<br>0072 | 0.0<br>072 |
| 46       | 0.0       | 0.0           | 0.0       | 4.6<br>4  | 0.0       | 0.0       | 9.2<br>5  | 0.0       | 0.0       | 0.0       | 13.90                  | 38.<br>34       | 2023-11-<br>11T13:40<br>:36.082            | 2023-11-<br>11T14:09<br>:08.330            | 0.0<br>06 | 0.0<br>06 | 0.0<br>06 | 0.0<br>06 | 0         | 0         | 0.0<br>06 | 0.0<br>06 | 0         | 0.0<br>06 | 0.00<br>0126 | 0.0<br>126 |
| 47       | 9.2<br>8  | 0.0           | 0.0       | 0.0       | 0.9<br>3  | 0.0       | 0.0       | 0.0       | 0.9<br>3  | 0.0       | 11.15                  | 35.<br>59       | 2023-11-<br>11T14:15<br>:01.192            | 2023-11-<br>11T14:40<br>:34.068            | 0.0<br>06 | 0         | 0.0<br>06 | 0         | 0.0<br>06 | 0         | 0.0<br>06 | 0.0<br>06 | 0.0<br>06 | 0         | 0.00<br>0108 | 0.0<br>108 |
| 48       | 0.0       | 4.6<br>4      | 0.0       | 0.0       | 0.0       | 0.0       | 0.0       | 9.2<br>7  | 0.0       | 0.0       | 13.92                  | 38.<br>36       | 2023-11-<br>11T14:45<br>:06.953            | 2023-11-<br>11T15:23<br>:18.578            | 0         | 0.0<br>06 | 0.0<br>06 | 0         | 0         | 0         | 0.0<br>06 | 0.0<br>06 | 0         | 0         | 0.00<br>0072 | 0.0<br>072 |
| 49       | 9.2<br>6  | 0.0           | 0.0       | 0.0       | 0.0       | 9.2<br>8  | 9.2<br>7  | 18.<br>55 | 9.2<br>8  | 0.0       | 55.65                  | 80.<br>09       | 2023-11-<br>11T16:00<br>:06.250            | 2023-11-<br>11T17:00<br>:15.344            | 0.0<br>06 | 0         | 0.0<br>06 | 0         | 0         | 0.0<br>06 | 0.0<br>06 | 0.0<br>06 | 0.0<br>06 | 0         | 0.00<br>0108 | 0.0<br>108 |
| 50       | 18.<br>56 | 0.0           | 0.0       | 0.0       | 0.0       | 18.<br>56 | 36.<br>98 | 0.0       | 0.0       | 0.0       | 74.11                  | 98.<br>55       | 2023-11-<br>12T08:15<br>:12.714            | 2023-11-<br>12T08:56<br>:17.563            | 0.0<br>06 | 0.0<br>06 | 0.0<br>06 | 0         | 0         | 0.0<br>06 | 0.0<br>06 | 0.0<br>06 | 0.0<br>06 | 0         | 0.00<br>0126 | 0.0<br>126 |
| 51       | 0.0       | 18.<br>56     | 18.<br>56 | 0.0       | 0.0       | 0.0       | 9.2<br>7  | 37.<br>12 | 0.0       | 0.0       | 83.53                  | 107<br>.96      | 2023-11-<br>12T09:10<br>:19.711            | 2023-11-<br>12T09:45<br>:23.482            | 0         | 0.0<br>06 | 0.0<br>06 | 0         | 0         | 0.0<br>06 | 0.0<br>06 | 0.0<br>06 | 0         | 0.0<br>06 | 0.00<br>0108 | 0.0<br>108 |
| 52       | 0.0       | 0.0           | 0.0       | 0.9<br>3  | 0.0       | 0.0       | 0.0       | 9.2<br>8  | 0.9<br>3  | 0.0       | 11.14                  | 35.<br>58       | 2023-11-<br>12T09:55<br>:08.844            | 2023-11-<br>12T10:33<br>:40.553            | 0         | 0.0<br>06 | 0.0<br>06 | 0.0<br>06 | 0         | 0         | 0.0<br>06 | 0.0<br>06 | 0.0<br>06 | 0         | 0.00<br>0108 | 0.0<br>108 |
| 53       | 0.0       | 0.0           | 0.0       | 0.0       | 4.6<br>4  | 0.0       | 9.2<br>6  | 0.0       | 0.0       | 0.0       | 13.91                  | 38.<br>34       | 2023-11-<br>12T10:44<br>:56.749            | 2023-11-<br>12T11:20<br>:37.606            | 0.0<br>06 | 0.0<br>06 | 0.0<br>06 | 0         | 0.0<br>06 | 0         | 0.0<br>06 | 0.0<br>06 | 0.0<br>06 | 0         | 0.00<br>0126 | 0.0<br>126 |
| 54       | 0.0       | 0.0           | 0.0       | 0.0       | 0.0       | 0.0       | 0.0       | 0.0       | 0.0       | 0.0       | 0.01                   | 24.<br>45       | 2023-11-<br>12T12:30<br>:00.602            | 2023-11-<br>12T13:00<br>:00.389            | 0.0<br>06 | 0         | 0.0<br>06 | 0.0<br>06 | 0         | 0         | 0.0<br>06 | 0.0<br>06 | 0         | 0.0<br>06 | 0.00<br>0108 | 0.0<br>108 |
| 55       | 0.0       | 0.0           | 0.0       | 1.8<br>6  | 0.0       | 0.0       | 0.0       | 0.0       | 0.0       | 0.0       | 1.87                   | 26.<br>31       | 2023-11-<br>12T13:05<br>:08.714            | 2023-11-<br>12T14:01<br>:43.871            | 0.0<br>06 | 0         | 0.0<br>06 | 0.0<br>06 | 0         | 0         | 0.0<br>06 | 0.0<br>06 | 0         | 0.0<br>06 | 0.00<br>0108 | 0.0<br>108 |
| 56       | 18.<br>56 | 18.<br>56     | 18.<br>56 | 18.<br>56 | 0.0       | 0.0       | 47.<br>50 | 92.<br>80 | 18.<br>56 | 0.0       | 233.1                  | .56             | 2023-11-<br>12T14:05<br>:14.356            | 2023-11-<br>12T14:11<br>:47.965            | 0.0<br>06 | 0.0<br>06 | 0.0<br>06 | 0.0<br>06 | 0         | 0         | 0.0<br>06 | 0.0<br>06 | 0.0<br>06 | 0         | 0.00<br>0126 | 0.0<br>126 |
| 57       | 0.0       | 0.0           | 0.9<br>3  | 0.0       | 0.0       | 0.0       | 0.0<br>1  | 4.6<br>4  | 0.0       | 0.0       | 5.58                   | 30.<br>02       | 2023-11-<br>12T14:30<br>:19.449            | 2023-11-<br>12T15:30<br>:22.073            | 0         | 0.0<br>06 | 0.0<br>06 | 0         | 0         | 0         | 0.0<br>06 | 0.0<br>06 | 0.0<br>06 | 0         | 0.00<br>009  | 0.0<br>09  |
| 58       | 0.9<br>3  | 0.0           | 0.0       | 0.0       | 0.0       | 0.9<br>3  | 0.0<br>1  | 0.0<br>1  | 0.0       | 0.0       | 1.87                   | 26.<br>31       | 2023-11-<br>12T15:41<br>:39.323            | 2023-11-<br>12T16:36<br>:42.637            | 0.0<br>06 | 0         | 0.0<br>06 | 0         | 0         | 0.0<br>06 | 0.0<br>06 | 0.0<br>06 | 0         | 0         | 0.00<br>009  | 0.0<br>09  |
| 59       | 7.4<br>2  | 0.0           | 0.0       | 0.0       | 0.0       | 7.4<br>3  | 0.0       | 37.<br>10 | 5.9<br>7  | 0.0       | 57.92                  | 82.<br>36       | 2023-11-<br>13T09:59<br>:23.510            | 2023-11-<br>13T10:39<br>:29.814            | 0.0<br>06 | 0         | 0.0<br>06 | 0         | 0         | 0.0<br>06 | 0.0<br>06 | 0.0<br>06 | 0.0<br>06 | 0         | 0.00<br>0108 | 0.0<br>108 |
| 60       | 7.4<br>3  | 0.0           | 0.0       | 0.0       | 0.0       | 7.4<br>2  | 0.0       | 37.<br>12 | 7.3<br>3  | 0.0       | 59.31                  | 83.<br>74       | 2023-11-<br>13T10:46<br>:02.401            | 2023-11-<br>13T11:15<br>:36.063            | 0.0<br>06 | 0         | 0.0<br>06 | 0         | 0         | 0.0<br>06 | 0.0<br>06 | 0.0<br>06 | 0.0<br>06 | 0         | 0.00<br>0108 | 0.0<br>108 |
| 61       | 7.4<br>2  | 0.0           | 0.0       | 0.0       | 0.0       | 7.4<br>2  | 0.0<br>1  | 37.<br>09 | 7.4<br>1  | 0.0       | 59.36                  | 83.<br>80       | 2023-11-<br>13T11:22<br>:27.678            | 2023-11-<br>13T11:52<br>:23.423            | 0.0<br>06 | 0.0<br>06 | 0.0<br>06 | 0         | 0         | 0.0<br>06 | 0.0<br>06 | 0.0<br>06 | 0.0<br>06 | 0         | 0.00<br>0126 | 0.0<br>126 |
| 62       | 9.2<br>8  | 0.9<br>3      | 0.0       | 0.0       | 0.9       | 0.0       | 18.<br>52 | 0.0       | 0.0       | 0.0       | 29.67                  | 54.<br>11       | 2023-11-<br>13T12:10<br>:01.424            | 2023-11-<br>13T12:38<br>:47.726            | 0.0<br>06 | 0.0<br>06 | 0.0<br>06 | 0         | 0.0<br>06 | 0         | 0.0<br>06 | 0.0<br>06 | 0.0<br>06 | 0         | 0.00<br>0126 | 0.0<br>126 |
| 63       | 0.9       | 0.0           | 3.7       | 0.0       | 0.0       | 0.0       | 0.0       | 25.<br>98 | 0.0       | 5.5<br>4  | 36.17                  | 60.<br>61       | 2023-11-<br>13T12:50<br>:20.478            | 2023-11-<br>13T13:19<br>:27.400            | 0.0<br>06 | 0         | 0.0<br>06 | 0         | 0         | 0         | 0.0<br>06 | 0.0<br>06 | 0         | 0.0<br>06 | 0.00<br>009  | 0.0<br>09  |
| 64       | 4.6<br>4  | 4.6<br>4      | 4.6<br>4  | 4.6<br>4  | 0.0       | 0.0       | 29.<br>59 | 0.0       | 4.6<br>4  | 0.0       | 52.80                  | 77.<br>24       | 2023-11-<br>13T14:30<br>:14.232            | 2023-11-<br>13T14:44<br>:02.286            | 0.0<br>06 | 0.0<br>06 | 0.0<br>06 | 0.0<br>06 | 0         | 0         | 0.0<br>06 | 0.0<br>06 | 0.0<br>06 | 0         | 0.00<br>0126 | 0.0<br>126 |
| 65       | 4.6<br>4  | 9.2<br>8      | 6.5<br>0  | 0.0       | 4.6<br>4  | 0.0       | 29.<br>64 | 0.0       | 0.0       | 4.6<br>3  | 59.33                  | 83.<br>77       | 2023-11-<br>13T15:59<br>:57.197            | 2023-11-<br>13T16:30<br>:01.065            | 0.0<br>06 | 0.0<br>06 | 0.0<br>06 | 0         | 0.0<br>06 | 0         | 0.0<br>06 | 0.0<br>06 | 0         | 0.0<br>06 | 0.00<br>0126 | 0.0<br>126 |
| 66       | 18.<br>56 | 0.0           | 0.0       | 18.<br>56 | 0.0       | 0.0       | 44.<br>41 | 0.0       | 0.0       | 0.0       | 81.54                  | 105<br>.98      | 2023-11-<br>14T08:15<br>:30.074            | 2023-11-<br>14T09:15<br>:35.680            | 0.0<br>06 | 0.0<br>06 | 0.0<br>06 | 0.0<br>06 | 0         | 0         | 0.0<br>06 | 0.0<br>06 | 0         | 0         | 0.00<br>0108 | 0.0<br>108 |
| 67       | 0.0       | 18.<br>56     | 18.<br>56 | 0.0       | 0.0       | 0.0       | 9.2<br>7  | 55.<br>68 | 0.0<br>1  | 0.0       | 102.0<br>7             | 126<br>.51      | 2023-11-<br>14T09:25<br>:33.216            | 2023-11-<br>14T10:25<br>:39.759            | 0         | 0.0<br>06 | 0.0<br>06 | 0.0<br>06 | 0         | 0         | 0.0<br>06 | 0.0<br>06 | 0         | 0         | 0.00<br>009  | 0.0<br>09  |
| 68       | 0.0       | 0.0           | 0.0       | 0.0       | 0.0       | 0.0       | 0.0       | 9.2<br>8  | 0.0<br>2  | 0.0       | 9.27                   | 33.<br>71       | 2023-11-<br>14T10:35<br>:03.583            | 2023-11-<br>14T11:35<br>:10.493            | 0         | 0         | 0.0<br>06 | 0         | 0         | 0         | 0.0<br>06 | 0.0<br>06 | 0         | 0         | 0.00<br>0054 | 0.0<br>054 |

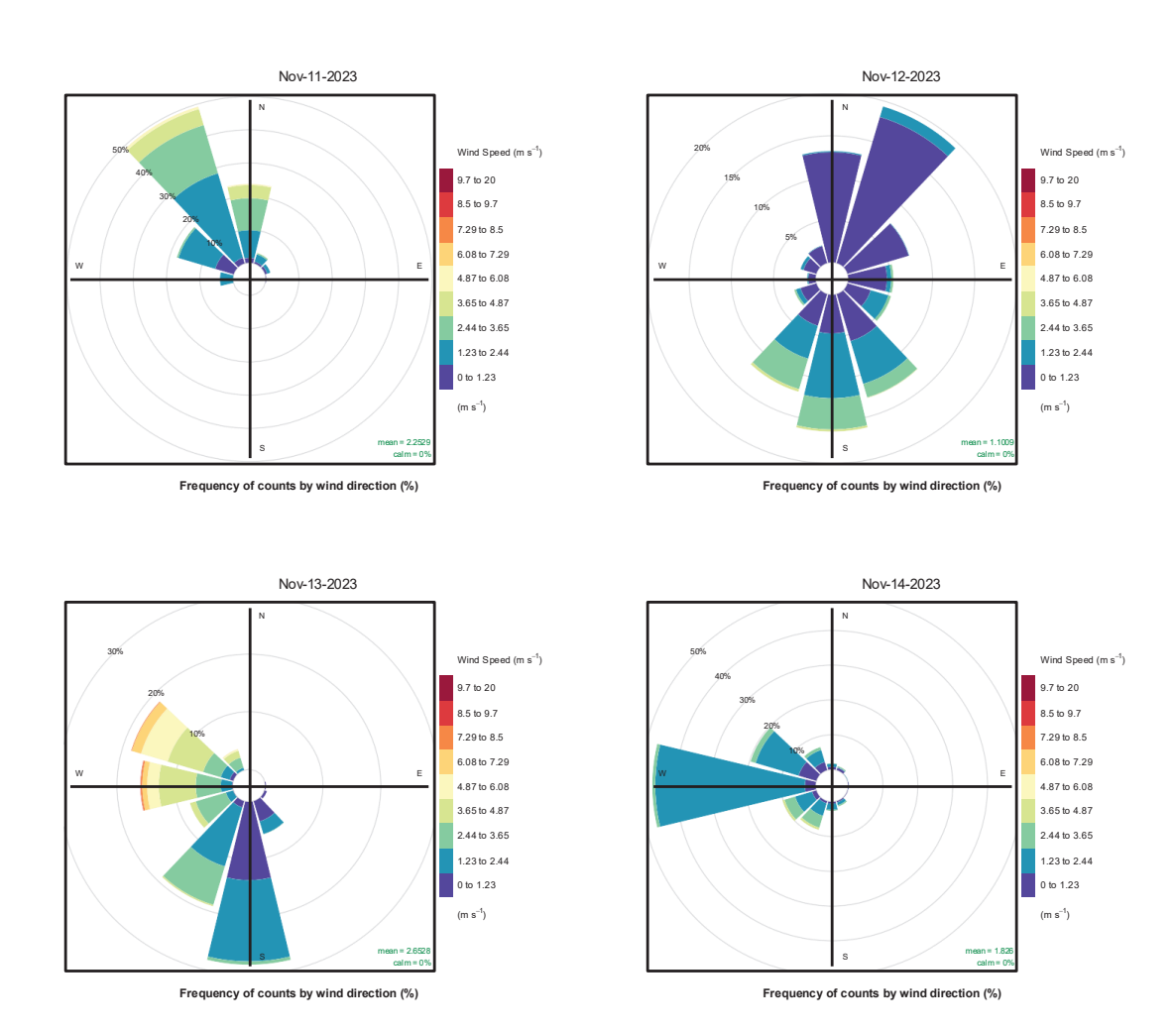
| Ex<br>p# | Q_<br>A   | Q_<br>B   | a <sup>l</sup> c | Q_<br>D1 | Q_<br>D2 | Q_<br>D3  | Q_<br>E   | Q <sub>-</sub> F | Q_<br>K4  | Q_<br>K5 | Flow<br>meter<br>Total | Sit<br>e<br>Tot<br>al | Time<br>Start                   | Time<br>End                     | U_<br>A   | U <sub>B</sub> | n_c       | Q_<br>D1  | Q_<br>D2  | Q_<br>D3  | Q_<br>E   | Q_<br>F   | Q_<br>K4  | Q_<br>K5 | RSS          | %U         |
|----------|-----------|-----------|------------------|----------|----------|-----------|-----------|------------------|-----------|----------|------------------------|-----------------------|---------------------------------|---------------------------------|-----------|----------------|-----------|-----------|-----------|-----------|-----------|-----------|-----------|----------|--------------|------------|
| 69       | 0.0       | 0.0       | 0.0              | 0.0      | 4.6<br>4 | 0.0       | 9.2<br>1  | 0.0              | 0.0<br>1  | 0.0      | 13.84                  | 38.<br>28             | 2023-11-<br>14T11:44<br>:55.704 | 2023-11-<br>14T11:53<br>:04.610 | 0         | 0.0<br>06      | 0.0<br>06 | 0         | 0.0<br>06 | 0         | 0.0<br>06 | 0.0<br>06 | 0         | 0        | 0.00<br>009  | 0.0<br>09  |
| 70       | 18.<br>56 | 18.<br>56 | 18.<br>56        | 0.0      | 0.0      | 18.<br>56 | 45.<br>90 | 99.<br>64        | 18.<br>56 | 0.0      | 238.3<br>4             | 262<br>.78            | 2023-11-<br>14T13:58<br>:06.401 | 2023-11-<br>14T14:09<br>:07.384 | 0.0<br>06 | 0.0<br>06      | 0.0<br>06 | 0         | 0         | 0.0<br>06 | 0.0<br>06 | 0.0<br>06 | 0.0<br>06 | 0        | 0.00<br>0126 | 0.0<br>126 |
| 71       | 0.0       | 4.6<br>4  | 0.0              | 0.0      | 0.0      | 0.0       | 0.0       | 9.2<br>8         | 0.0       | 0.0      | 13.93                  | 38.<br>37             | 2023-11-<br>14T14:29<br>:54.462 | 2023-11-<br>14T15:59<br>:55.332 | 0         | 0.0<br>06      | 0.0<br>06 | 0.0<br>06 | 0         | 0         | 0.0<br>06 | 0.0<br>06 | 0.0<br>06 | 0        | 0.00<br>0108 | 0.0<br>108 |

Table S5: Mass flowrates and associated uncertainty of all experiments. Timings are listed in local time (ET).

Wind and meteorological conditions



# Figure S5. Daily wind roses from November 5 to November 10 from the Eastern meteorological station. Station locations are shown in Figure S8.



1047

Figure S6. Daily wind roses from November 11 to November 14 from the Eastern meteorological station. Station locations are shown in Figure S8.

Weather Station ELARS

Weather Station HARS

Wind Speed (m/s)
9 to 10
8 to 9
7 to 8
6 to 7
6 to 6
4 to 5
3 to 4
2 to 3
1 to 2
0 to 1
(m/s)

mean = 2 3088

Frequency of counts by wind direction (%)

1050

1051

1052

1053

1054

1055

1056

1057

1058

1059

Frequency of counts by wind direction (%)

Wind Speed (m/s)

10 to 13.74

# Weather Station NARS Wind Speed (m/s) 10 to 12.05 9 to 10 8 to 9 7 to 8 6 to 7 5 to 6 4 to 5 3 to 4 2 to 3 1 to 2 0 to 1 (m/s)

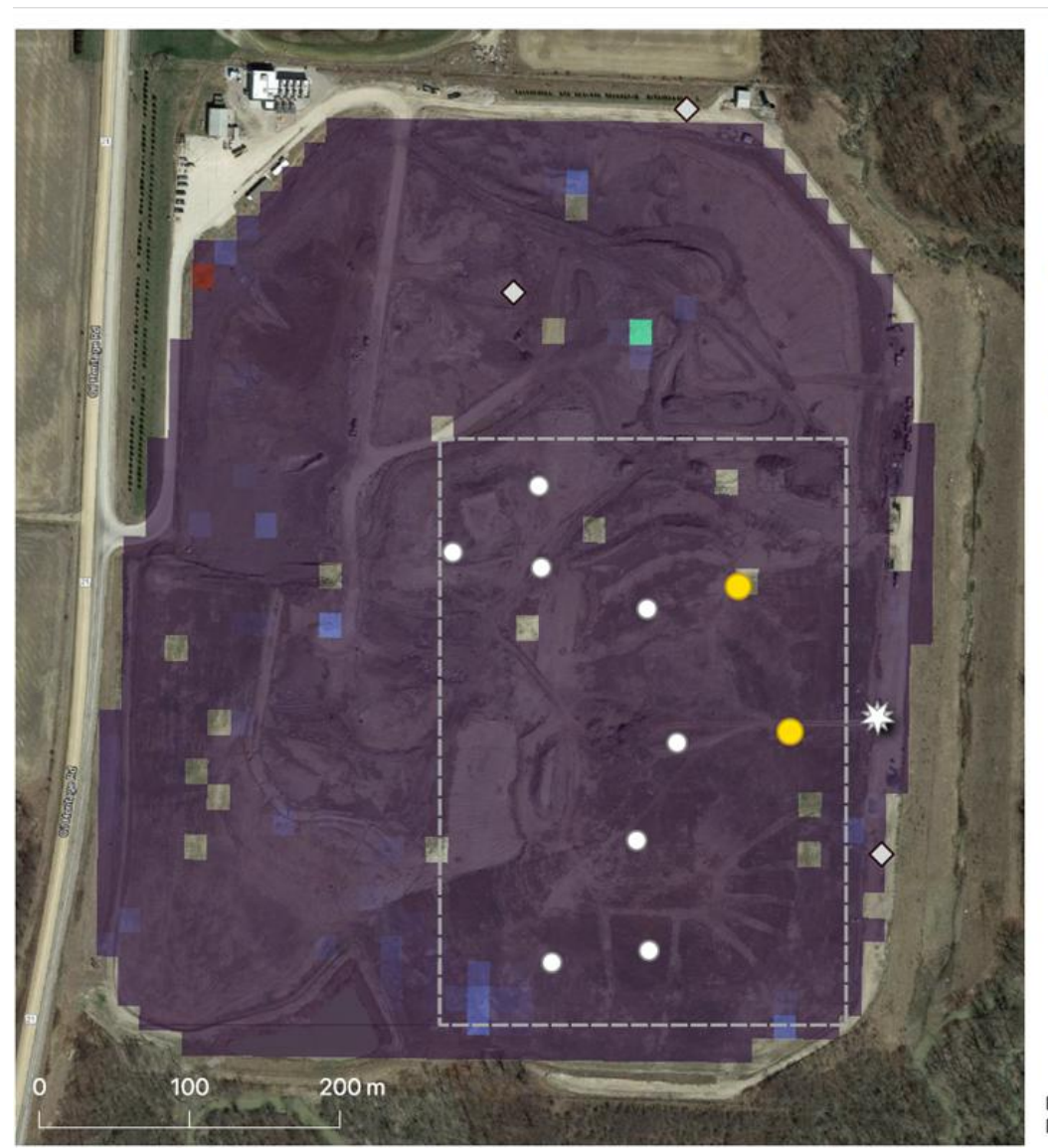
Frequency of counts by wind direction (%)

Figure S7: Windrose charts of Eastern, Hilltop and Northern Atmospheric Research Stations. Station locations are shown in Figure S8.

# **Site Configuration**



Figure S8: Map of controlled release configuration.



# Legend

Weather Stations

Gas Truck

**Detection Facility** Release Points

Diffuse Release Areas

Surface Emission Monitoring Band 1: z (Gray)

800

Basemap: Google Maps Projection: NAD83 (CSRS) UTM Zone 17N

Figure S9: Walking SEM concentration map of the search area

1073

1074